國立臺灣大學生命科學學院動物學研究所

碩士論文

Graduate Institue of Zoology
College of Life Science
National Taiwan University

Master Thesis

探討 *Dj*Ago2 蛋白在渦蟲再生中所扮演的角色

Study on the role of Argonaute protein *Dj*Ago2 in planarian regeneration

張智凱

Chi-Kai Chang

指導教授：朱家瑩 博士

Advisor: Chia-Ying Chu, Ph.D.

中華民國 101 年 2 月

February, 2012

國立臺灣大學碩士學位論文
口試委員會審定書

探討*Dj*Ago2蛋白在渦蟲再生中所扮演的角色
Study on the role of Argonaute protein *Dj*Ago2 in planarian regeneration

本論文係張智凱君（R98b41032）在國立臺灣大學動物學系、所完成之碩士學位論文，於民國101年1月31日承下列考試委員審查通過及口試及格，特此證明

口試委員：

（簽名）

（指導教授）

動物學研究所所長 （簽名）

致謝

從前總是覺得致謝這樣的文章，在畢業的時候一定是信手拈來，隨處是感謝的字句。然而在經過了這段不知是長還是短的時間後，回首一盼，要感謝的人和事真是多到不知該如何下筆。首先要感謝的當然是朱家瑩老師的細心指導，不論是實驗還是做人處世上，老師常強調的邏輯性思考、辨明是非、待人有禮，都成為是大家為人處世的標竿。還要感謝老師在實驗方向的修正、論文內容改正上的勞心勞力，更在忍受了我不成熟的實驗技術、不足的闡述能力以及癟腳的英文寫作能力之餘，仍能不厭其煩的給予指導及教導。感謝陳俊宏老師、李心予老師、詹世鵬老師，在研究方向上給予意見，以及口試和論文修改上給予很大的幫助。感謝羅竹芳老師、齊肖琪老師、于宏燦老師，在我剛進學校時給予的建議。謝謝台大科技共同空間的莊以君學姊、楊亞臻學姊、高毓鄖學姊、蕭君儀學姊、阿湯哥，沒有你們的大力協助和被煩卻又逃不掉的意氣，我的實驗無法順利進行。還有要感謝李心予老師實驗室的 Milky 學長、沛翊學長、易謙學姊、翠華學姊、傳恩、耆豪、岳謙、予農，常去麻煩你們和借藥品。感謝羅竹芳老師實驗室的詩婷學姊、怡婷學姊教我進行 miRNA 的實驗。感謝陳俊宏老師實驗室的岱威、亞凡、政儀、哈哈、尚樺、易澤，常去找你們詢問無脊椎動物的問題和實驗方法，當然也借了很多小東西。感謝吳益群老師實驗室的學長姐贊助抑制基因表現的方法。感謝丘臺生老師實驗室的志翔學長的大力協助，並且讓我們可以常常去你們那邊聊天。最後要感謝實驗室的夥伴們，勁文學長的樂觀和勤勉是在遇到挫折時鼓舞著我，讓我得到前進的動力。感謝本崔學長、芷均、妍君、郁文、捥恕陪伴著我的實驗室生涯，並且讓實驗室總是處於沸騰的狀態。還有大學部學弟妹，弘毅、翊柔、若晞、方怡、意清，解決你們的問題有時卻能藉此整理自己的思緒和認識自己。最後的最後，感謝家人的支持與諒解，這段時間雖然無法參加並幫忙處理家裡的事物，但我心與你們同在，也感謝你們與我同在。

摘要

渦蟲是一種具有再生能力的扁形動物，能由身體一部分片段再生出包含腦部的完整個體。渦蟲的再生能力建立在一群多功能成體幹細胞(neoblast)身上，他們可以進行複製以及分化來替換身體所有的組織，而且這群細胞對 γ-射線很敏感。*Dugesia japonica*(東洋渦蟲)的 *Dj*Ago2 蛋白是人類 Ago2 的同源蛋白質，在人類細胞上的研究顯示 *hs*Ago2 是 miRNA 和 siRNA 路徑中的關鍵因子，具有調控基因表現的能力。本研究中，我們首先選殖 *Dj*Ago2 之完整全長 cDNA 並構築與 YFP 蛋白接合之重組蛋白表現載體，將其表現在 HeLa cell 中。在螢光顯微鏡下觀察發現，*Dj*Ago2 會和人類的 P-body 組成物 RCK 等聚集於細胞質內，這現象和 *hs*Ago2 的表現很類似。藉由整體原位雜交的實驗，發現 *Djago2* 高度表現在渦蟲的頭部和背中線上。渦蟲尾部再生的實驗中顯示在 blastema 以及 post-blastema 兩區 *Djago2* 的表現量在再生時會上升，而 RT-qPCR 的結果也顯示其表現量在再生第三天的 blastema 和 post-blastema 中，分別高出平常的五倍和兩倍。藉由 FACS 來分離 neoblast 和已分化細胞，發現 *Djago2* 在成體幹細胞中的表現量較高，而且 γ-射線會使得部分表現 *Djago2* 的細胞消失。最後，用 *Djago2* dsRNA 來餵食渦蟲以抑制蟲體中 *Djago2* 的表現，渦蟲會失去再生的能力而且會喪失組織恆定性。RT-qPCR 的結果顯示表現在幹細胞 (*DjpiwiA*)以及合成 DNA (*Djpcna*) 的基因表現量在抑制 *Djago2* 後會下降。而且，M phase 的細胞減少以及 G2 phase 的細胞增加顯示抑制 *Djago2* 會使得成體幹細胞的細胞周期停留在 G2 phase 而無法進行有絲分裂。同時，也觀察到部分渦蟲出現分化受到限制的現象。我們的實驗結果顯示，*Djago2* 在渦蟲成體幹細胞的細胞複製、自我更新以及分化時都被需要的，可以藉由對於成體幹細胞的調控來影響渦蟲的再生能力。

關鍵字：

渦蟲、再生、成體幹細胞、微核醣核酸

Abstract

Planarians are capable of regenerating almost every part of their body, including the brain. Regeneration in planarians is mediated by a group of pluripotent adult somatic stem cells, called neoblasts, which can proliferate and differentiate to replace all tissues. These cells are sensitive to γ-irradiation. *Dj*Ago2 of *Dugesia japonica* is a homolog of *hs*Ago2, the key factor that regulates gene expression in miRNA and siRNA pathways. In the study, *DjAgo2* was cloned, and YFP-tagged *Dj*Ago2 was expressed in HeLa cells. *Dj*Ago2 accumulates at specific foci that contain the P-body component, RCK. This pattern is similar to what we observed with *hs*Ago2. By whole-mount *in situ* hybridization (WISH), *Djago2* was found to be highly expressed in regions of the brain and the middle dorsal line. *Djago2* expression was increased in the blastema and post-blastema during regeneration. RT-qPCR results confirmed that respective *Djago2* mRNA expression levels in the blastema and post-blastema were 5 and 2-times higher than that in the control at 3 days post-amputation. WISH data showed that a portion of *Djago2*-positive cells were depleted by γ-irradiation. We next examined *Djago2* expression levels in neoblasts isolated by FACS. Our RT-qPCR data showed that the *Djago2* level was higher in neoblasts than that in differentiated cells. Finally, *Djago2* was silenced by feeding planarians *Djago2* dsRNA. Depletion of *Djago2* resulted in loss of the regeneration capacity and defects in tissue homeostasis in planarians. *Djago2* silencing reduced levels of *DjpiwiA, Djpcna,* and *DjpiwiC*. Our data also showed that the ratio of M-phase cells was decreased and the ratio of G2-phase cells was increased in *Djago2*-silenced animals. This suggests that *Djago2* silencing blocked the mitosis of neoblasts. Differentiation restriction was also observed in *Djago2*-silenced animals. Our data indicate that *Djago2* is required for neoblast proliferation, and differentiation.

Keyword:

Planarian, regeneration, neoblast, Ago2, miRNA

Contents

1. Introduction

1.1 Planarians and regeneration

Planarians are bilaterally symmetric metazoans in the class Turbellaria of the phylum Platyhelminthes. Planarians are small unsegmented flatworms that are not parasitic. They are commonly found in freshwater ponds or streams, and move by cilia on the ventral dermis. Planarians are triploblastic and acoelomate, which means they have three embryonic tissue layers, including an ectoderm, mesoderm, and endoderm, without a body cavity. While planarians have no specific circulatory, respiratory, or skeletal structures, they do have a digestive system with a pharynx and a blind gut, but no anus (Salo and Baguna, 2002). Planarians have a simple visual system on their heads. The visual system includes a pair of eyespots with rhabdomeres and pigment cells (Sakai et al., 2000). The photoreceptors can sense light intensity and directionality but form no images (Sakai et al., 2000).

The regeneration ability of planarians is remarkable. A small amputated fragment from any part of their body can regenerate to form a complete worm (Morgen, 1901). Studies on planarian regeneration were initiated several hundred years ago. Peter Simon Pallas was the first person to describe how a small piece of amputated planarian head

has the capability to regenerate to an intact body in 1766 (Brøndsted, 1969). Experiments on planarian regeneration were performed by Dalyell and Johnson in the early nineteenth century. According to their results, Dalyell concluded that planarians may “almost be called immortal under the edge of the knife” (Brøndsted, 1969). After that, Harriet Randolph defined the minimal size of a fragment capable of regeneration as 1/279 of an intact worms (Randolph, 1897).

Thomas Hunt Morgan was the first person to systematically study planarian regeneration (Morgen, 1901). He described the regenerative ability and polarity of planarian regeneration. Although many animals can regenerate missing tails, arms, or legs, the planarian is one of the few animals that can even regenerate a head. In planarians, a new head is formed in 7 days after transverse amputation of the region posterior to the pharynx. New eyes are formed in 4 days of head regeneration. Therefore, it is a valuable model system for elucidating mechanisms that control cell and tissue replacement, a process that is important for the survival of most organisms (Slack, 2011).

Various species of planarians were characterized in detail as having either asexual or sexual strains. Some of them are commonly used to study regenerative phenomena in biological laboratories. For example, *Dugesia ryukyuensis* has been shown to exhibit the

capability of switching from asexual to sexual reproduction (Hoshi et al., 2003). The freshwater hermaphrodite, *Schmidtea mediterranea,* was well characterized by Alvarado's group in the past 10 years, and has emerged as a model system. In this study, I use *Dugesia japonica* as a model planarian. It is commonly distributed in the Far East, including Japan, Taiwan, Korea, China, and Primorskiy in Russia (Tamura et al., 1998). In addition, *D. japonica* is the only species of freshwater planarian in Taiwan. The karyotype of *D. japonica* can be diploid, triploid, or mixoploid (Tamura et al., 1998). For many research groups in Asia, *D. japonica* has become a suitable model system for studying the regeneration and developmental processes at the cellular and molecular levels.

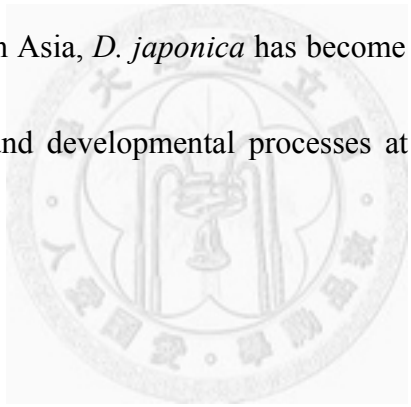

1.2 Blastema and neoblasts

During planarian regeneration, lost parts of the body are rebuilt from the remaining tissues. The process of regeneration includes at least two events: blastema formation and pattern formation. The blastema is the pigment-free bud formed at a wound site after amputation. After blastema formation, cells in the newly grown tissues then differentiate into different cell types according to the developmental signals that determine the body's polarity. T.H. Morgan, who was the first researcher to perform

many experiments to understand how polarity is reestablished after amputation (Morgen, 1901). Recent studies showed that some signaling pathways regulate the dorsal-ventral axis and anterior-posterior polarity during regeneration. For example, *SmedBmp4-1* molecules in the BMP signaling pathway are expressed in the midline region of intact animals, and regulate dorsal-ventral patterning (Reddien et al., 2007). *SmedWntP-1*, expressed in a few cells in the tail of intact animals, regulates anterior-posterior (AP) polarity during regeneration (Petersen and Reddien, 2009). Knockdown of the gene expression of β-catenin leads to ectopic heads at wound sites in all body regions (Adell et al., 2009; Chai et al., 2010; Gurley et al., 2008; Petersen and Reddien, 2008).

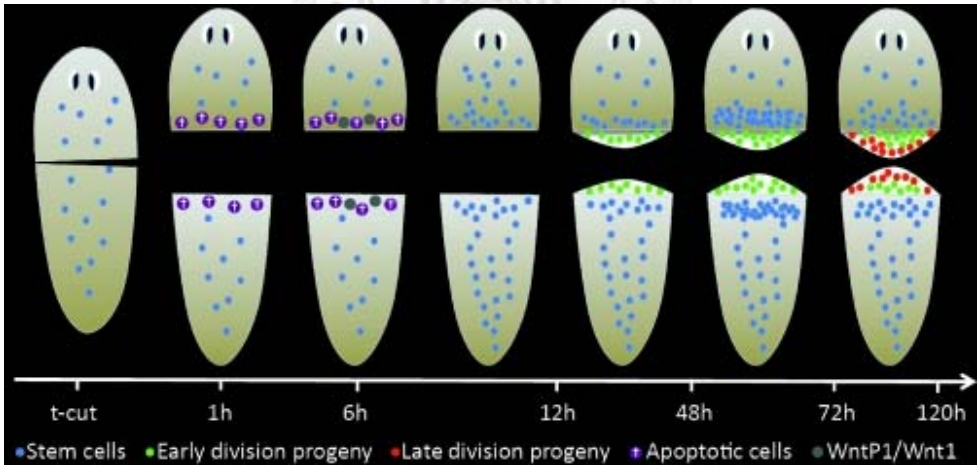

(Gentile et al., 2011)

Source cells of the blastema were investigated for decades (Baguna and Romero, 1981; Slack, 1980). It is now accepted that the blastema is formed by proliferation of pluripotent stem cells, called neoblasts (Baguna et al., 1989). Neoblasts are small cells

of 5~10 μm. Neoblasts has a large nucleus surrounded with a thin cytoplasmic layer. Many studies indicated that the blastema is not the proliferation site of neoblasts in planarians. During regeneration, cell division occurs in the region next to the blastema, called the post-blastema. It seems that damaged nerve fibers may release regulatory molecules into the extracellular space to regulate the process of regeneration(Salo and Baguna, 1984, 1989), even though no molecular evidence was shown. Cell proliferation of neoblasts is activated during regeneration. An early mitotic peak from slowly dividing cells with a long G2 phase, is observed at 8~12 h after amputation. The early mitotic peak reflects the existence of parts of neoblasts in the G2 phase, which await an appropriate signal to divide. The second mitotic peak occurs 2~4 days after amputation. After cell proliferation, neoblasts migrate to the blastema and differentiate into various cell types. This process of restoring the amputated body part to an intact animal is completed within 2~3 weeks (Baguna et al., 1989).

Neoblasts fit the classical definition of a stem cell. They are small undifferentiated cells and are required for normal growth, self-renewal, and regeneration in planarians (Eisenhoffer et al., 2008). Neoblasts are localized in the parenchyma which lies beneath the muscle and surrounds the organs. Neoblasts comprise about 20%~30% of planarian cells, but only a small percentage of them have the capability for mitotic division

(Baguna and Romero, 1981; Baguna et al., 1989). Some of them are the immediate division progeny of neoblasts (Eisenhoffer et al., 2008). Neoblasts are described as adult stem cells, but they are unlike adult stem cells of mammals. In mammals, a tissue contains a small number of tissue-specific stem cells through which it can continuously renew itself. Fetal and adult stem cells are usually multipotent and can differentiate into limited cell types. However, the neoblasts of planarians are pluripotent stem cells that can renew all types of differentiated cells, whereas only mammalian embryonic stem cells exhibit pluripotency.

X-ray irradiation was used to inhibit planarians' regenerative abilities by eliminating stem cells with mitotic ability (Bardeen and Baetjer, 1904). Wolff and Dubois performed serial experiments, with various portions of an animal shielded from irradiation (Wolff 1962). If the anterior region of an intact animal was irradiated and the region was amputated, the irradiated region became necrotic and died. The un-irradiated fragment of the same animal survived. If the anterior region of an intact animal was irradiated and the head was removed, the irradiated region was repaired and blastema was formed with a regeneration delay. This regeneration delay reflects neoblasts having to migrate through the irradiated region to the wound site. Therefore, planarians are like a culture dish. Although X-ray-irradiated planarians lose their regenerative ability,

transplantation of a neoblast-enriched cell population into irradiated animals can restore their regenerative ability (Baguna et al., 1989; Wagner et al., 2011). It indicates the regenerative ability of planarians depends on the neoblasts.

Planarians with developmental plasticity have the capability to grow and 'de-grow' depending on the nutritional status (Baguna and Romero, 1981; Lillie, 1900). A full-grown adult (~20 mm long) can shrink to a size that is much smaller (~1 mm) after starvation for months (Newmark and Sanchez Alvarado, 2002). Growth and de-growth in planarians occur due to changes in cell numbers (Baguna and Romero, 1981), not from changes in cell size. It is thought that the ratio of cells born by proliferation to cells lost by apoptosis changes during starvation. The phenotype of irradiated animals is similar to that of starved animals, which indicates that the activity of neoblasts is important for tissue homeostasis.

The mechanism of blastema formation in planarians differs from that of vertebrates. First, wound epithelium is formed by epidermal cell shape modifications in planarians, but it forms by cell proliferation in vertebrates. Second, mesenchymal cells are from preexisting neoblasts in planarians, but are from dedifferentiated cells in vertebrates (Newmark 2001). Parenchyma cells accumulate as neoblasts in the blastema (Betchaku, 1967, 1970), and the cytoplasmic processes of fixed parenchyma cell are related to

directional movements of regenerative cells by providing a contact guidance system (Hori, 1991). This indicates that differentiated cells regulate the behavior of adult stem cells by an extracellular substance.

For regeneration research, biologists tried to label these cells. Thymidine and 5'-bromo-2'-deoxyuridine (BrdU) are used to label cycling cells. Serine 10 of histone H3 becomes phosphorylated throughout condensing chromatin at the initiation of mitosis. Anti-H3P is used to label cells in the M phase (Hendzel et al., 1997). Recently, increasing numbers of genes were found in neoblasts. *Djmcm2* is a member of the minichromosome maintenance (MCM) family of DNA replication factors (Salvetti et al., 2000). *DjPCNA* is a component of the DNA replication protein complex (Orii et al., 2005). *DjRbAp48* is a component of different chromatin-modeling complexes (Bonuccelli et al., 2010). All three of those genes are specifically expressed in neoblasts and strongly expressed in the dorsal midline. *Djvas-1*, *Djpabpc-1*, and *DjpiwiA* are components of RNA granules, and are expressed in neoblasts (Rouhana et al., 2010). Neoblasts can also be detected and isolated by fluorescence activated cell sorting (FACS) (Hayashi et al., 2006).

Several genes are known to be required for neoblast maintenance, e.g., *Smedwi-2* (Reddien et al., 2005), *Smedwi-3* (Palakodeti et al., 2008), *Smed-bruli* (Guo et al., 2006),

Dj-pum (Salvetti et al., 2005), *Spoltud-1* (Solana et al., 2009), *Smed-SmB* (Fernandez-Taboada et al., 2010), *Smedinx-11* (Oviedo and Levin, 2007), *Djmot* (Conte et al., 2009), and *Smed-CHD4* (Scimone et al., 2010). Several genes are found in progenitor cells, e.g., *Smed-AGAT1*, *Smed-NB21.11e* (Eisenhoffer et al., 2008), and *Smed-p53* (Pearson and Sanchez Alvarado, 2010). Silencing of these gene blocks the regenerative ability in planarians. According to those studies, we know that planarian regeneration depends on the presence and precise regulation of neoblasts, which differentiate to replace cells of any missing tissue (Rouhana et al., 2010). After over 200 years of studies, the mechanism of planarian regeneration is still unclear. But there are many markers to monitor the stages of neoblasts for research on planarian regeneration.

1.3 Small RNAs in planarian

In 1998, experimental introduction of RNA into cells can be used in certain biological systems to interfere with the function of an endogenous gene. In recent years, small, non-coding RNAs were shown to be essential players in almost all biological processes. Small RNAs (siRNA, miRNA, piRNA, tncRNA, snRNA) have the ability to regulate gene expressions in animal development, regeneration, stress response, and transposon silencing. Many small-RNA species have been identified. But most of the

biological functions of these species are still unclear. The miRNAs are endogenous RNAs with ~22 nucleotides that can play important regulatory roles in animals and plants by targeting mRNAs for cleavage or translational repression (Bartel, 2004). Recently, functions of miRNAs were identified to be involved in regulation of cell cycle, cell proliferation, cell death, apoptosis, and fat metabolism in Drosophila (Brennecke et al., 2003), neuronal patterning in nematodes (Johnston and Hobert, 2003), and development of leaf and flower in plants (Aukerman and Sakai, 2003; Palatnik et al., 2003). miRNAs are also important to stem cells. Some miRNAs are specifically expressed in human and mouse embryonic stem cells (Houbaviy et al., 2003; Suh et al., 2004), and miRNAs have the ability to regulate the differentiation of hematopoietic stem cells in mice (Chen et al., 2004) and germline stem cells in *Drosophila* (Hatfield et al., 2005). Previous studies suggested that 90% of genes may be regulated by miRNAs in humans (Miranda et al., 2006).

The mature miRNAs are produced from precursor transcripts called primary miRNAs by RNA polymerase II (Cai et al., 2004; Lee et al., 2002). The pri-miRNA is processed into a 60~70-nucleotide pre-miRNA by Drosha in the nucleus (Lee et al., 2003). Pre-miRNAs have a two-nucleotide overhang at their 3' ends and a 5' phosphate group. Pre-miRNA is cleaved by Dicer to generate a duplex of miRNA and miRNA*

(Schwarz et al., 2003). Dicer is component of the RISC loading complex. RISC loading complex recruits Ago2 and transfers the miRNA duplex. Ago2 can then cleave the target RNA or repress translation (Kim et al., 2007; Liu et al., 2004). Most miRNAs pair with their targets through the sequence at the 5' end from the second to the eighth called the "seed region" (Brennecke et al., 2005; Lewis et al., 2005). A single miRNA therefore can regulate many different mRNAs, whose sequences are complementary to seed region in miRNA (Lewis et al., 2003).

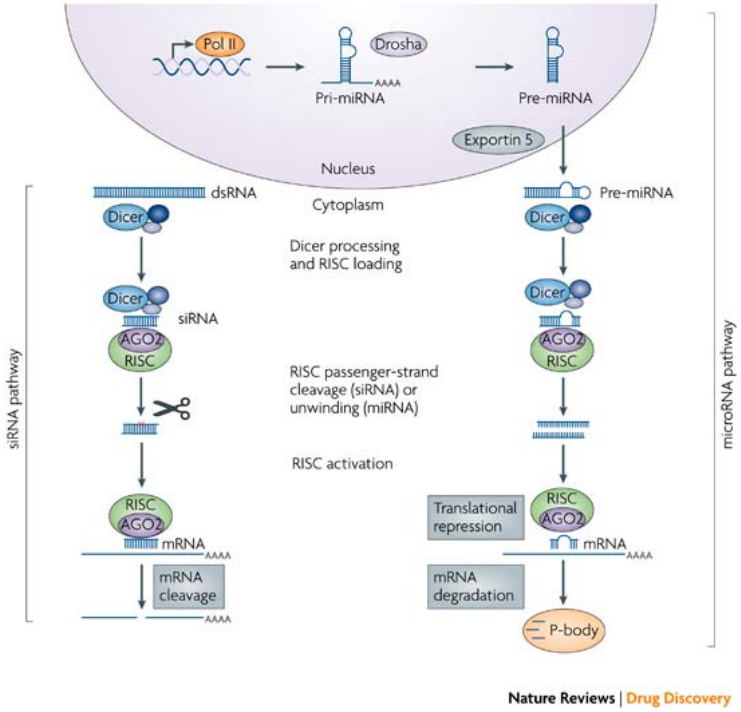

(Farrar et al., 2011)

The piRNAs are the longest small RNAs with 25~32 nucleotides and they function in the germ line. Unlike siRNAs, piRNAs are mainly antisense. This suggests that piRNAs are produced from long, single-stranded precursor RNAs. Biogenesis of piRNA

is from sequences of piRNAs that are bound to Piwi, Aubergine and Ago3 (Brennecke et al., 2007). The biogenesis of piRNA occurs through an amplification mechanism of "ping-pong" that is activated after transcription of transposon mRNA (Tabara et al., 2002). In planarians, miRNAs and piRNAs are predominant small RNAs (Friedlander et al., 2009).

Dasaradhi Palakodeti et al was the first group to study miRNAs in planarian. They reported the cloning and initial characterization of 71 miRNAs from the planarian *Schmidtea mediterranea* (Palakodeti et al., 2006). Marc R. Friedländer et al used massive, next-generation sequencing methods to compare profile of small RNAs present in neoblasts, irradiated animals, and normal animals (Friedlander et al., 2009). The read numbers of piRNAs were predominant in sorted neoblasts (82%), and low in the irradiated sample (25%) (Friedlander et al., 2009). In contrast, miRNAs were predominant in the irradiated sample, but several miRNAs were enriched in neoblasts. They used a reverse transcription quantitative polymerase chain reaction (RT-qPCR) to confirm the deep sequencing data. Ten miRNAs were up-regulated in neoblasts (let-7a, let-7b, miR-36b, miR-2a, miR-2d, miR-13, miR-71b, miR-756, and miR-2160). Yi-Chien Lu et al used the same method to define the full complement of small RNAs present in irradiated animals, un-irradiated animals, a sexual strain, and an asexual

strain. Five miRNAs were identified that were reduced by at least 2-fold in irradiated animals (let-7a, mir-71b, mir-756, mir-13, and mir-752) (Lu et al., 2009). Qing-Nan Tian et al identified 8 miRNAs that were differentially expressed in regenerative tissues using an miRNA microarray (miR-71a, miR-756, miR-13, miR-281, miR-79, miR-2d-3p, miR-36, and miR-2b) (Tian et al., 2011). Cristina González-Estévez et al showed that 12 miRNAs were sensitive to irradiation by small RNA whole-mount *in situ* hybridization (WISH) (let-7c, mir-2c, mir-71c, mir-67, mir-2d, mir-71b, mir-752, mir-7b, mir-36, mir-92, mir-124a, and mir-124b) (Tian et al., 2011). Those results indicated that miRNAs might play important roles in regeneration or neoblast maintenance and differentiation.

1.4 Argonaute proteins

The Argonaute protein family was first identified in plants, and were later found in bacteria, archaea, and eukaryotes (Cerutti and Casas-Mollano, 2006) . They are highly conserved among species, and many organisms encode multiple members of the family (Hock and Meister, 2008). Members of this family are defined by having a Piwi-Argonaute-Zwille (PAZ) domain and a P-element induced wimpy testis (PIWI) domain (Bohmert et al., 1998). Studies on Ago2 structure have shown that the PAZ

domain has a subdomain which displays oligonucleotide binding (OB)-like folding. It also showed that the PAZ domain can recognize 3' ends of single-stranded RNAs (Yan et al., 2003). The Mid domain is between the PAZ and PIWI domains and has cap-binding activity. The PIWI domain binds to the 5' end of siRNA and the target RNA. The PIWI domain contains catalytic residues (DDH) with the capacity (Song et al., 2004) to cleave the mRNA strand between nucleotides 10 and 11 if the complementarity of the miRNA and mRNA is perfect (Yuan et al., 2005).

The Argonaute protein family has two subfamilies, the Argonaute and PIWI. The Argonaute subfamily is similar to *Arabidopsis thaliana* Ago1, while the PIWI subfamily is similar to *Drosophila melanogaste*r PIWI (Carmell et al., 2002). Argonaute subfamily proteins are expressed and bind to siRNAs or miRNAs for post-transcriptional gene silencing either by translational repression or by destabilization of the mRNA. PIWI proteins are involved in piRNA pathway. The mechanism of PIWI proteins is not clear. In planarians, several PIWI proteins were identified. *Smedwi-2* and S*medwi-3* have the ability to regulate neoblast proliferation (Palakodeti et al., 2008). *Drpiwi-1* is essential for germline cell formation during sexualization of the planarian *Dugesia ryukyuensis* (Nakagawa et al., 2012). The Argonaute protein was identified in planarians. *Djago2* silencing results in a failure to regenerate (Rouhana et al., 2010). However, the role of

Djago2 in planarian regeneration is still unclear.

2. Materials and Methods

2.1 Animals

The planarian *D. japonica* was captured in Jiaoxi Township, Ilan County, of northeastern Taiwan. The worms were maintained in aerated tap water at 18 °C for at least a month and fed chicken liver once a week. Replacement of the aerated tap water three times a week was used to control water quality. In this study, worms were used after 1 week of starvation.

2.2 5’ Rapid amplification of complementary (c)DNA ends (RACE) and 3’RACE

Total RNA was collected from intact planarians with the TRIzol reagent. 5' RACE-PCR began using mRNA as a template for a first round of cDNA synthesis with the superscript III First-strand Synthesis System (Invitrogen). An anti-sense gene-specific primer was used to recognizes *Djago2* mRNA template in the 3' to 5' direction to generate a specific single-stranded cDNA product. Following cDNA synthesis, the enzyme terminal deoxynucleotidyl transferase (TdT), was used to add a string of deoxycytidine triphosphates (dCTPs) to the 3' end of the cDNA. A PCR reaction was performed using a secondary antisense gene-specific primer and an oligo

(dG) primer. The products of the PCR were cloned into a TA vector and sequenced. The 3' RACE-PCR used an oligo (dT) primer to generate cDNA. The PCR was then used to amplify 3' cDNA using a sense gene-specific primer and an oligo (dT) primer. The products of the PCR were cloned into the TA vector and sequenced. The first antisense gene-specific primer was GCATAATAAGCAGGAGCTGG, the secondary antisense gene-specific primer was CCGTCAAACACAGGTCTCTG, and the sense gene-specific primer was GGTGTTTGGGATATGAGAGG.

2.3 Expression vectors

Expression vectors with N-terminal YFP-tag was generated by PCR amplification of Expression vectors with an N-terminal yellow fluorescent protein (YFP) tag was generated by PCR amplification of *Djago2* coding sequences from cDNA of intact planarians, followed by cloning into the XhoI and BamHI sites of pEYFP-C1 (BD).

2.4 Cell culture and transfection

HeLa cells were cultured in Dulbecco's minimal essential medium (DMEM) with 10% fetal bovine serum (FBS) at 37 °C with 5% CO_2. Cells were transfected using Lipofectamine (Invitrogen) according to the manufacturer's protocol.

2.5 Immunofluorescence

Cells transfected with YFP-*Djago2* were fixed with 4% paraformaldehyde in phosphate-buffered saline (PBS) at room temperature for 20 min and permeabilized for 5 min with 0.25% (v/v) Triton X-100. Samples were washed three times with PBST (0.1% [v/v] Triton X-100 in PBS) and blocked for 30 min in PBST containing 2% (w/v) bovine serum albumin (BSA). Primary and secondary antibodies were diluted in blocking solution during incubation. Antibodies used in these experiments included anti-RCK/p54 and anti-YFP. Secondary antibodies against rabbit and mouse immunoglobulin G (IgG) were directly conjugated to Alexa Fluor dyes (Molecular Probes, Eugene, OR). Samples were washed three times with PBST after antibody incubation. After the final wash, samples were counterstained with Hoechst 33342 to visualize nuclei.

2.6 Whole mount *In situ* hybridizations

Animals 5 to 8 mm long were used for this experiment. Planarians were killed, and mucus was removed with 5% N-acetyl cysteine in 5/8 Holtfreter's solution for 5 min on slides, and then specimens were fixed in 4% formaldehyde for 20 min. Worms were

transferred into 1.5ml Eppendorf-tubes. Fixed samples were washed with 50% methanol and 100% methanol, and bleached overnight in methanol with 6% H_2O_2. Animals were washed with a serial dilution of methanol: PBST (0.3% triton X-100 in PBS). Animals were treated with 2 μg/ml of a proteinase K solution. Worms were then incubated at 56 °C for 2 h in pre-hybridization solution (50% formamide, 5× SSC, 1% Tween-20, and 1 mg/ml yeast torula RNA). Hybridization was performed at 65 °C in hybridization solution containing 50% formamide, 10% dextran sulfate, 5× SSC, 1% Tween-20, and 1 mg/ml yeast torula RNA with a DIG-labeled antisense RNA probe for 16 h. Animals were washed through a serial dilution into 2x SSC, then 0.2x SSC, and finally into MABT (100 mM maleic acid, 150 mM NaCl, and 0.1% Tween-20; pH 7.5). Animals were incubated with blocking solution (10% goat serum in MABT) for 2 h, and then with primary antibodies (1:4000 anti-digoxigenin-AP (Roche) diluted in blocking solution) overnight. Animals were washed 6 times with MABT, and the signal was developed with an NBT/BCIP mixture.

2.7 Preparation of single-cell suspensions for the fluorescence-activated cell sorting (FACS) analysis

Planarians were cut into three fragments on ice, and rinsed with a calcium- and

magnesium-free solution (CMF: 2.56 mM $NaH_2PO_4 \cdot H_2O$, 10.21 mM KCl, 14.28 mM NaCl, 9.42 mM NaHCO3, and 1% BSA). The fragments were cut into smaller pieces and treated with 0.25% (w/v) trypsin in CMF for several minutes at room temperature. Samples were completely dissociated into single cells by gentle pipetting and then filtered through a 70-μm-pore size cell strainer (BD) and a 20-μm nylon net filter (Millipore) to remove tissue fragments. The single-cell suspensions were incubated with 13.5 μg/mL Hoechst 33342 (Sigma) and 0.5 μg/mL calcein-*AM* (Sigma) for 1 h at room temperature. Samples were pelleted by centrifugation at 1500 g for 2 min, and resuspended in CMF. A flow cytometric analysis used a FACSAria III cell sorter (BD).

2.8 Quantitative PCR

Total RNA was extracted using TRIzol, and cDNA was synthesized with the superscript III First-strand Synthesis System (Invitrogen). A real-time RT-PCR was performed using SYBR® FAST qPCR Kits (KAPA). *Djactin* was used for normalization. The following primers were used in the amplification reaction:

Djago2 forward, 5'-CCTGTAATATTTCTCGGTGCTGA-3';

Djago2 reverse, 5'-CATCCATACTGCCTACAACAGC-3';

Djactin forward, 5'-GGTAATGAACGATTTAGATGTCCAGAAG-3';

Djactin reverse, 5'-TCTGCATACGATCAGCAATACCTGGAT-3';

DjpiwiA forward, 5'-GGAGCCATAGGAGAAATCTCATTTG-3';

DjpiwiA reverse, 5'-CGCTAATCCAAATCCGGGAAC-3';

DjPCNA forward, 5-TGAGGCTATCACCATTACTGTTG-3';

DjPCNA reverse, 5'-GGCTCGGTCATTTCAATAGTG-3';

DjpiwiC forward, 5-GGACGTGACTACTTCTACCCAG-3';

DjpiwiC reverse, 5'-CTTTGTGTGAAACATCGCACTG-3'

2.9 RNA interference (RNAi) experiments

Double-stranded (ds)RNA was used to knock down *Djago2* expression (Sanchez Alvarado and Newmark, 1999). The *Djago2* dsRNA sequence was cloned by a PCR. The following primers were used: forward primer, GCCTAATACGAGACACTAT-AGAAGGTGTTTGGGATATGAGAGG; and reverse primer, GCCTAATACGAC-TCACTATAGGGTAACAATGCCGAAATTTGAT. These primers had a T7 promoter sequence. *Djago2* dsRNA was synthesized with T7 polymerase for 3 h. After RNA synthesis, the sample was digested with DNase I for 15 min at 37 °C. *Djago2* dsRNA was precipitated with ethanol, and resuspended in 20 μl of nuclease-free H_2O. Formation of dsRNA was confirmed by running 200 ng of these reactions in a 1.0%

agarose gel in TAE. This artificial food was mixed with 4 μg dsRNA in 25 μl of a 75% chicken liver mix, 6 μl 2% ultra-low gelling agarose, and 1 μl red food color. The artificial food mix was allowed to solidify at 4 °C, and room-temperature food was fed to planarians. Worms were fed with RNAi food on days 1, 4, and 7. After the 3rd RNAi feeding, the heads and tails were immediately removed. After 9 days of regeneration, animals were fed and amputated again. The phenotype was monitored by a dissecting microscope.

2.10 Anti-phospho-histone H3 labeling

To detect mitotic cells, a rabbit anti-phospho histone H3 antibody (Millipore) was used to detect mitotic cells. Planarians were killed by ice-cold 2% HCl (0.5~1 min) and then fixed in Carnoy's solution for 2.5~3 h at room temperature. After rinsing in MeOH, fixed specimens were bleached overnight in 6% H_2O_2 in MeOH at room temperature. Planarians were either stored at -20 °C in MeOH or immediately rehydrated through an MeOH/PBSTx (0.3% Triton X-100 in PBS) series (75%, 50%, and 25% MeOH). Samples were blocked and incubated overnight at room temperature in anti-H3P diluted 1:1000 in PBSTx + 10% goat serum. After multiple PBSTx washes (for at least 8 h), samples were post-fixed for 15 min at room temperature in 4% paraformaldehyde in

PBS and washed twice in PBSTx. Samples were incubated overnight at 4 °C in anti-rabbit Alexa 488 (1:1000) diluted 1:1000 in PBTx + 10% goat serum. Following three 10-min washes in PBSTx, samples were stained with Hoechst 33342 for 30 min.

3. Results

3.1.1 Cloning of Planarian Argonaute - *Djago2*.

The full length sequence of *Djago2* was completed by 5'RACE and 3'RACE. The clone with 2787 nucleotides was isolated and sequenced (Fig.1B). The initial methionine was identified by comparison with the sequences of AGO2 ortholog from other organisms. The *Djago2* encodes a protein composed of 929 amino acids. Phylogenetic analysis showed *Dj*Ago2 is a member of AGO subfamily and is closely related to *Schmidtea mediterranea* Ago2, *Drosophila melanogaster* Ago1 and human Ago2 (Fig. 1A). *Dj*Ago2 contains conserved PAZ, Mid and PIWI domains. Sequence alignment of *Dj*Ago2 with its ortholog in humans, hsAgo2, showed that is exhibited high similarity to human Ago2 with 76.5% identity, especially in the PIWI domain (88%) (Fig.1B). *Dj*Ago2 also contains DDH, which are key residues for the catalytic activity of Ago2.

3.1.2 The subcellular distribution of *Dj*Ago2 is similar to that of human Ago2 localized to P-bodies.

To characterize if the cloned *Dj*Ago2 indeed exhibits similar function to its human

orthologue, I first examined localization of *Dj*Ago2 in HeLa cells. Previous studies showed that Ago2 is localized to cytoplasmic mRNA P-bodies, and facilitates miRNA-induced gene silencing. Therefore, I hypothesized that if DjAgo2 is the functional planarian Argonaute protein, it should also localize to P-bodies. YFP-tagged *Dj*Ago2 was expressed in HeLa cells, and its localization was confirmed by the human P-body marker, RCK/p54 (Fig 2). YFP-*Dj*Ago2 was expressed in cytoplasm, and accumulated at specific foci. RCK and YFP antibodies were used to label endogenous RCK and YFP-*Dj*Ago2. HeLa cells which expressed YFP-*Dj*Ago2 were co-stained with anti-YFP and anti-RCK. YFP-*Dj*Ago2 co-localized with endogenous RCK (Fig. 2, panels a, b, c). This expression pattern is similar to that of human Ago2 (Fig 2, panels d, e, f)

3.2.1 Expression pattern and level of *Djago2* in planarian.

To examine the expression of *Djago2* in intact planarians, I used WISH to detect the mRNA of *Djago2*. WISH for *Djago2* was performed with a digoxigenin-labeled antisense RNA probe. The RNA probe with ~1500 nucleotides in sequence length included the 3' UTR and a partial sequence of the PIWI domain. Animals that were 5~8 mm long were used for this experiment. A sense RNA probe was used as the control,

and no signal was detected after hybridization (Fig. 3A). This showed that the background signal was undetectable in our WISH system. The expression pattern of *Djago2* was detected in the whole body and was readily detected in central nervous system (CNS) and middle dorsal line. The expression pattern of *Djago2* in intact planarians was similar to *Djcbc-1* (*Dμgesia japonica chromatoid body component 1*) (Yoshida-Kashikawa et al., 2007). *Djcbc-1* is a homolog of human RCK/p54. In planarians, *Djcbc-1* is located in chromatoid bodies of neoblasts and chromatoid body-like structures in the CNS (data not shown). *DjpiwiA* is known to be a neoblast-specific gene, which is expressed throughout the planarian body. It is also expressed in cell clusters in the middle dorsal line (Fig. 3B).

3.2.2 *Djago2* is highly expressed in the regenerating region.

I next examined the expression of *Djago2* in regenerating animals. After amputation anterior and posterior to the pharyngeal region, the head, trunk, and tail were allowed to simultaneously regenerate. Expression patterns of *Djago2* in the head, trunk, and tail were observed on day 3 after transverse amputation. *Djago2* was expressed in cells of the CNS, middle dorsal line, and regenerating tissues (Fig. 4A). This showed that *Djago2* might be expressed in neoblasts. To observe *Djago2* levels at

wound sites during planarian regeneration, worms were transversely amputated posterior to the pharynx, harvested and analyzed by WISH. Animals were harvested at various time points of 8 h, and 1, 2, 3, 5, and 7 days after amputation. Expression of *Djago2* was increased in the regenerating region during regeneration until 3 days, and the signal was lower on day 5 and 7 (Fig. 4B).

The expression levels of *Djago2* at various regeneration time points were quantified by RT-qPCR. During planarian regeneration, the regenerating tissue, called the blastema, contains a mass of cells which is capable of replacing lost or damaged body parts. In previous studies, *DjpiwiA*-labeled neoblasts proliferated in the region of the post-blastema and then migrated to and differentiated into various cell types in the blastema (Umesono et al., 2011). Quantitative analysis of *Djago2* was performed for tissues of the blastema and post-blastema during regeneration. Blastemas were harvested at various time points of 3, 5, and 7 days after transverse amputation at the post-pharyngeal region. Post-blastema samples of three more time points at 8, 24, 48 h post-amputation were harvested in the regenerating region. Expression levels of *Djago2* were not examined in the blastema at 3, 5, or 7 days post-amputation because the newly formed tissues were too small. Control samples of the blastema and post-blastema were the tail and the region next to the first amputation, respectively. In total, 2 μg of RNA in

each sample was collected for reverse transcription to produce cDNA and was subjected to a qPCR analysis. In the post-blastema, expression of *Djago2* was increased during regeneration, and *Djago2* was respectively 2.5- and 3.2-fold higher than the control at 8 and 72 h post-amputation (Fig. 5A). In the blastema, expression of *Djago2* was 6-fold higher than the control at 72 h post-amputation (Fig. 5B). Our results showed that the expression of *Djago2* was increased in both the blastema and post-blastema during regeneration. Then I examined expression levels of *DjpiwiA*, a marker for neoblasts, in the blastema at 3, 5, and 7 days post-amputation. Expression of *DjpiwiA* did not rise up at 72 h after the first amputation (Fig. 5C). On days 5 and 7 post-amputation, expression levels of *DjpiwiA* were lower than the control. This confirmed that neoblasts had accumulated in the post-blastema but not in the blastema during regeneration.

3.3.1 γ-irradiation eliminates the *Djago2*-positive cells.

Since the increasing expression of *Djago2* in regenerating tissues was synchronized with that of *DjpiwiA*, I hypothesized that *Djago2* is expressed in neoblasts, and *Djago2* expression is higher as a result of proliferation and differentiation of neoblasts. To check if *Djago2* is expressed in neoblasts, I examined expression levels of *Djago2* in both normal and neoblast-depleted animals. I depleted neoblasts in planarians by 90 Gy

γ-irradiation. Fourteen days after γ-irradiation, all animals displayed degeneration (Fig. 6A). All animals were dead at 3~4 weeks after irradiation, indicating a failure of tissue homeostasis. I used FACS to confirm if γ-irradiation eliminated neoblasts (Fig. 6B). Single-cell suspensions were collected and filtered from dissociated animals. Staining with Hoechst 33342 reflects the DNA content in nuclei. The cytoplasm of living cells was stained with vital calcein-AM. In FACS, I first selected a population of particles which contained Hoechst 33342/calcein-AM double-positive cells. I separated those cells into three populations according to the DNA content and cell size. G2/M- (Fig 6B, p3) and G1/G0-phase cells (Fig. 6B, p4 and p5) could be distinguished by the Hoechst 33342 fluorescence signal. Our data showed that G2/M-phase cells (p3 in Fig 6B), which are highly proliferating neoblasts, had been eliminated at day 3 post γ-irradiation (Fig. 6B).

RT-qPCR analysis was used to examine the either *Djago2* or *DjpiwiA* expression levels between irradiated and un-irradiated animals. Total RNA was collected from three animals in different treatments. A total 3μg RNA was collected from three animals and used for cDNA preparation. Our results showed that γ-irradiation eliminated the expression of *DjpiwiA* and reduced the level of *Djago2* down to 23% as compared to the control. This demonstrated that γ-irradiation had eliminated neoblasts and reduced

Djago2 expression in intact animals (Fig. 6C). I also compared *Djago2* expression patterns between irradiated and un-irradiated animals by WISH (Fig. 7A). *Djago2* was expressed in the CNS in both irradiated and un-irradiated animals. But the detected signals were weaker in the intact bodies of irradiated worms. Interestingly, signals in cell clusters of the dorsal middle line were totally eliminated by γ-irradiation, suggesting that irradiation indeed depleted *Djago2*-positive neoblasts in the dorsal middle line. Comparing the expression of *Djago2* in irradiated and un-irradiated animals on day 3 post amputation, I found that the increased expression of *Djago2* near the wound site had disappeared as well (Fig. 7B).

3.3.2 *Djago2* is highly expressed in neoblasts.

To confirm the expression of *Djago2* in highly proliferating neoblasts, I collected G2/M-phase cells and analyzed their *Djago2* levels by an RT-qPCR. Single-cell suspensions were prepared from 60 worms at ~1.5 cm in length for the FACS analysis. Cells in population 3 (in the G2/M phase) were sorted as neoblasts. Cells in population 5 (in the G0/G1 phase) were sorted as differentiated cells. Cells in population 4, which contained part of the neoblasts, were not sorted. In total, 300 ng RNA was collected and subjected to cDNA synthesis. I compared *Djago2* and *DjpiwiA* expressions between

neoblasts and differentiated cells. The *Djago2* expression level was higher in neoblasts (Fig. 8).

3.4.1 Failure to regenerate in *Djago2*-silenced animals.

From previous data, I already knew that the *Djago2* expression level is higher in regenerating tissue, and *Djago2* is highly expressed in neoblasts. To check the function of *Djago2* in planarian regeneration, I knocked down *Djago2* by administering dsRNA. I observed loss of the head and tail formation in planarian regeneration with one round of *Djago2* dsRNA feeding, but not in control animals (Fig. 9B). Pleiotropic regeneration defects were observed in *Djago2*-knocked down planarians. Fifteen of 30 trunks were observed to have no blastema formation on day 7 after transverse amputation in the anterior and posterior regions of the pharynx (Fig. 9C). Seven of 30 trunks were observed to have limited regeneration with a single photoreceptor or no photoreceptor formation on day 7 after amputation. I extended the observation period to 14 days. Three of seven trunks had formed a complete photoreceptor, others had formed an incomplete photoreceptor, while five of 30 animals died. In control animals, 29 of 30 trunks regenerated to intact animals, and one trunk died (Fig. 9C). Higher knockdown efficiency was observed by increasing the feeding times of *Djago2* dsRNA (data not

shown), while I also found that animals began degenerating at the head region. However, most trunks did regenerate and died when I fed them *Djago2* dsRNA more than five times.

I examined the expression of *Djago2* in animals that had failed to regenerate by an RT-qPCR. The expression level of *Djago2* was reduced to 11% after *Djago2* silencing. Expression levels of *DjpiwiA*, *DjpiwiC*, and *Djpcna* were also reduced to 3%, 16%, and 17% at 7 days after amputation (Fig. 9C). This suggested that depletion of *Djago2* may eliminate a large population of neoblasts and also that *Djago2* is required for maintaining the homeostasis of neoblasts.

I therefore checked if neoblasts were indeed eliminated in *Djago2*-depleted worms using a FACS analysis. Surprisingly, the FACS results showed that cells of population 3 (in the G2/M phase) were not depleted in animals that had failed to regenerate (Fig. 9D). Moreover, the percentage of G2/M-phase cells had increased in animals that had failed to regenerate (Fig. 9E), suggesting that an undefined mechanism may be involved in the regenerating deficiency phenotype of *Djago2*-depletion.

For those animals which showed incomplete regeneration with *Djago2* RNAi, I further checked the pattern of formation of the head region to understand if *Dj*Ago2 is also required for differentiation. *Djndk* is a head marker in planarians used to show the head

formation in control and limited-regeneration (RNAi) animals 14 days after amputation. I examined expression patterns of *Djndk* by WISH. Compared to control RNAi animals, incomplete head formation was observed in *Djago2* RNAi-treated animals (Fig. 10). This result suggested that the differentiation potential from neoblast progeny was restricted in *Djago2* RNAi-treated animals.

3.4.2 Tissue homeostasis defect was observed in long-term *Djago2* RNAi-treated animals.

As mentioned above, I observed the head-regression phenotype when I increased the *Djago2* dsRNA feeding rounds. I therefore increased the dsRNA concentration in the RNAi food (6 mg of dsRNA in 25 μl of liver) to check if this degeneration phenotype resulted from the complete knockdown of *Djago2*. The head-regression phenotype was observed when RNAi food was given 3 to 6 times (Fig. 11A). This phenotype was similar to that of irradiated animals (Fig 6A). I examined the expression of *Djago2* in head-degenerated animals by an RT-qPCR. The *Djago2* expression level was reduced to 57%. Respective expression levels of *DjpiwiA* and *Djpcna* were reduced to 43% and 40% (Fig. 11B). These results suggested dysfunction of neoblasts in *Djago2* RNAi-treated animals.

Since neoblasts are the only mitotic cells in planarians as far as is known, I labeled mitotic cells with anti-phospho-histone 3-serine 10 (H3P), to confirm if the depletion of *Djago2* affected the M-phase of mitosis. As shown in Fig. 11C, numbers of H3P-positive cells dramatically decreased in *Djago2*-silenced animals. However, cell cytometric data showed that G2/M-phase cells were not significantly reduced in degenerating animals (Fig. 11D). Similar to animals that had failed to regenerate (Fig. 9E), the ratio of G2/M-phase cells even increased in degenerating animals compared to the control (Fig. 11E). A summary of these results indicated that RNAi of *Djago2* blocked dividing neoblasts.

4. Discussion

4.1 *Dj*Ago2 is a member of the Argonaute subfamily.

Argonaute proteins are highly conserved in many organisms. Members of the Argonaute protein family are characterized by the presence of PAZ (Piwi-Argonaute-Zwille), Mid, and PIWI domains. The protein sequence of *Dj*Ago2 is most similar to *Drosophila* Ago1 and human AGO2, and *Dj*Ago2 has homology to the Argonaute subfamily (Fig. 1). The PAZ domain of *Dj*Ago2 has 79.7% identity with *Drosophila* Ago1 and 75.7% identity with human AGO2. The PIWI domain of *Dj*Ago2 has 84.8% identity with *Drosophila* Ago1 and 85.8% identity with human AGO2. The PAZ domain is bound to the 3' end of small RNA. The PIWI domain is bound to the 5' end of small RNA. This shows that *Dj*Ago2 might have small RNA-binding affinity. The PIWI domain of *Dj*Ago2 contains the catalytic residue, DDH, which is an essential motif for cleavage activity. This indicates that *Dj*Ago2 potentially has mRNA-cleavage activity. In *Drosophila*, Ago1 functions in the miRNA-mediated translation repression pathway (Miyoshi et al., 2005), and Ago2 plays major roles in the RNAi pathway. Both of them have slice activity, and are involved in different pathways. The protein sequence of *Dj*Ago2 is more closely related to *Drosophila* Ago1 than to Ago2, suggesting that the

function of *Dj*Ago2 is more related to miRNA pathways. In addition, I found that when YFP-tagged *Dj*Ago2 was expressed in HeLa cells, it also localized to P-body and co-localized with human RCK, a P-body component (Fig. 2). Since human Ago2 is localized to cytoplasmic P-bodies which are mRNA decapping and degradation sites (Hutvagner and Simard, 2008). Our result suggests that *Dj*Ago2 might have a role in miRNA-mediated mRNA degradation.

4.2 *Djago2* is up regulated in regenerating tissue during planarian regeneration.

The expression level of *Djago2* increased at the wound site (Fig. 4A). During regeneration, the expression level of *Djago2* increased in the regenerating region from 8 hours to 3 days after amputation, and then decreased (Fig. 4B). In a quantification analysis, regenerating tissue was separated into two regions: the blastema and post-blastema. Post-blastema tissue contains many neoblasts which proliferate and differentiate into progenitor cells. These cells migrate to the blastema, and then differentiate into various types of differentiated cells. In the blastema, progenitor cells do not undergo mitosis. During regeneration, the expression of *Djago2* was increased 2.5-fold at 8 h post-amputation, and then had declined to 1.7-fold higher than the control at 48 h post-amputation (Fig. 5B). The expression of *Djago2* reached a peak at

72 h post-amputation (Fig. 5B). This phenomenon is similar to the change in neoblast proliferative activity during regeneration(Salo and Baguna, 1984). The increased level of *Djago2* is caused by the aggregation and proliferation of neoblasts. In the blastema, the expression of *Djago2* had increased to 6-fold higher than the control at 72 h post-amputation, and then dropped back to the control level (Fig. 5C). In the blastema, elevation of *Djago2* may be caused by a wound response of differentiated cells or the differentiation of progenitor cells. To clarify if the increase of Djago2 is a result of wound response or a signal from progenitor cells, we examine the expression level of *Djago2* at 72 h post amputation in irradiated animals. The expression of *Djago2* was not higher in irradiated animals on day 3 post-amputation (Figs. 4A, 7B). Therefore, the increased level of *Djago2* did not result from a wound response of differentiated cells, but from differentiation of progenitor cells.

4.3 Expression level of *Djago2* is higher in neoblasts than in differentiated cells.

My data show that *Djago2* is expressed in clustering cells which are located in the middle dorsal line (Fig. 2A). *DjpiwiA* is also expressed in the middle dorsal line (Fig. 3C). FACS data showed that 90 Gy of γ-irradiation eliminated neoblasts (Fig. 7B), while *Djago2*-positive cells in the middle line were also eliminated. RT-qPCR data

confirmed these results. The eliminated cells were neoblasts. The expression level of *Djago2* was lower in irradiated animals (Fig. 6C) and was higher in neoblasts (Fig. 8).

4.4 *Djago2* is required for proliferation of neoblasts and differentiation of progenitor cells.

In my data, three phenotypes were observed in *Djago2*-silenced animals. First, failure of regeneration was observed after *Djago2* RNAi food was administered 3 times (Fig. 9B). Parts of the trunk could not form a blastema at the wound site, and animals died within 14 days after amputation. This phenotype was similar to silencing of *Djbruli*, *Smedwi-2, Smed-smB (Fernandez-Taboada et al., 2010)*, *DjPCNA (Orii et al., 2005)*, and *DjRbAp48(Bonuccelli et al., 2010).* No blastema formation means no neoblasts or no proliferation. In *Djago2* RNAi worms, expression levels of *DjpiwiA*, *Djpcna,* and *DjpiwiC* were lower on day 7 post-amputation (Fig. 9D) with no blastema formation compared to control animals. *DjpiwiA* and *DjpiwiC* were used as neoblasts markers. The number of neoblasts decreased in *Djago2*-silenced animals.

In the second phenotype, parts of trunk fragments could form a blastema, but failed to form a pair of normal photoreceptors. This phenotype was similar to those of *Djcbc-1* and *Djtrans-2a*. This indicates that *Djago2* may be required for differentiation of

progenitor cells. Animals exhibiting limited head regeneration with a single photoreceptor were used to examine the ability of progenitor cells to differentiate. In a comparison of expression patterns of *Djndk* between normal animals and *Djago2* RNAi-treated animals, an incomplete brain was observed in animals with only one photoreceptor (Fig. 10). This indicated that *Djago2* silencing limited the differentiation capability of progenitor cells. However, we still need to check which types of differentiated cells can't be formed from progenitor cells in *Djago2* silenced animals. The regeneration of many organs other than brain also needs to be monitored to confirm that *Djago2* silencing limits the ability of progenitor cells to differentiate to other terminally differentiated cells (Oviedo and Levin, 2007).

In the third phenotype, homeostasis defects were observed when dsRNA was fed more than 3 times. Levels of *DjpiwiA*, *Djpcna,* and *DjpiwiC* decreased in both degenerating and regeneration-failed animals. Surprisingly, our FACS data showed that the number of G2/M-phase cells was increased in failed-regeneration animals (Figs. 9F, 11E). Since the mitotic cells can be also labeled by anti-H3P antibody, we found that the amounts of anti-H3P-positive cells were reduced in homeostasis-defective animals (Fig. 11C). This shows that *Djago2* silencing blocked the mitosis of neoblasts. It implied that, in *Djago2*-silenced animals, the cell cycle of neoblasts was stopped in the G2 phase.

These data suggest that head regression is resulted from a deficiency of neoblasts. My data showed that *Djago2* silencing led to animal regression and death, which might have been caused by apoptosis (Naoghare et al., 2011).

Taken together, our data suggest that *Djago2* is required for planarian regeneration and tissue homeostasis. *Djago2* is also required for proliferation and self-renewal of neoblasts and differentiation of progenitor cells (Fig. 12). In previous studies, inhibition of many RNA granule components, including *Djbruli*, *Djvas-1*, *Djcbc-1*, *Djupf-1*, *Djxrn-1*, *Djedc-4, Djdicer* and translation initiation factors, leds to lethality or limited regeneration (Anderson and Kedersha, 2006; Rouhana et al., 2010). This suggests that post-transcriptional regulators are required for stem-cell proliferation and planarian regeneration. Since *Djago2* is an orthologue of *hsago2* with high conservation, it is possible that *Djago2* also mediates small RNA-mediated gene silencing that regulates neoblast proliferation and progenitor cell differentiation. In the future, involvement of *Djago2* in planarian miRNA- or siRNA-mediated gene regulation should be further confirmed. We expect to identify the miRNAs regulated by *Djago2* in planarians by the immunoprecipitation of *Djago2*. In my preliminary data, several miRNAs were found to be up-regulated in regenerating tissue. We will further confirm if these miRNAs are associated with *Djago2*, and are required for planarian regeneration. Many following

experiments, such as using miRNA inhibitors to block the function of miRNA in planarians, will be conducted in the near future.

5. References

Adell, T., Salo, E., Boutros, M., and Bartscherer, K. (2009). Smed-Evi/Wntless is required for beta-catenin-dependent and -independent processes during planarian regeneration. Development *136*, 905-910.

Anderson, P., and Kedersha, N. (2006). RNA granules. J Cell Biol *172*, 803-808.

Aukerman, M.J., and Sakai, H. (2003). Regulation of flowering time and floral organ identity by a MicroRNA and its APETALA2-like target genes. Plant Cell *15*, 2730-2741.

Baguna, J., and Romero, R. (1981). Quantitative-Analysis of Cell-Types during Growth, Degrowth and Regeneration in the Planarians Dugesia-Mediterranea and Dugesia-Tigrina. Hydrobiologia *84*, 181-194.

Baguna, J., Salo, E., and Auladell, C. (1989). Regeneration and Pattern-Formation in Planarians .3. Evidence That Neoblasts Are Totipotent Stem-Cells and the Source of Blastema Cells. Development *107*, 77-86.

Bardeen, C.R., and Baetjer, F.H. (1904). The inhibitive action of the Roentgen rays on regeneration in planarians. Journal of Experimental Zoology *1*, 191-195.

Bartel, D.P. (2004). MicroRNAs: genomics, biogenesis, mechanism, and function. Cell

116, 281-297.

Betchaku, T. (1967). Isolation of planarian neoblasts and their behavior in vitro with some aspects of the mechanism of the formation of regeneration blastema. J Exp Zool *164*, 407-433.

Betchaku, T. (1970). The cellular mechanism of the formation of a regeneration blastema of fresh-water planaria, Dugesia dorotocephala. I. The behavior of cells in a tiny body fragment isolated in vitro. J Exp Zool *174*, 253-279.

Bohmert, K., Camus, I., Bellini, C., Bouchez, D., Caboche, M., and Benning, C. (1998). AGO1 defines a novel locus of Arabidopsis controlling leaf development. EMBO J *17*, 170-180.

Bonuccelli, L., Rossi, L., Lena, A., Scarcelli, V., Rainaldi, G., Evangelista, M., Iacopetti, P., Gremigni, V., and Salvetti, A. (2010). An RbAp48-like gene regulates adult stem cells in planarians. J Cell Sci *123*, 690-698.

Brøndsted, H.V. (1969). Planarian regeneration. Pergamon Press. Oxford.

Brennecke, J., Aravin, A.A., Stark, A., Dus, M., Kellis, M., Sachidanandam, R., and Hannon, G.J. (2007). Discrete small RNA-generating loci as master regulators of transposon activity in Drosophila. Cell *128*, 1089-1103.

Brennecke, J., Hipfner, D.R., Stark, A., Russell, R.B., and Cohen, S.M. (2003). bantam

encodes a developmentally regulated microRNA that controls cell proliferation and regulates the proapoptotic gene hid in Drosophila. Cell *113*, 25-36.

Brennecke, J., Stark, A., Russell, R.B., and Cohen, S.M. (2005). Principles of microRNA-target recognition. PLoS Biol *3*, e85.

Cai, X., Hagedorn, C.H., and Cullen, B.R. (2004). Human microRNAs are processed from capped, polyadenylated transcripts that can also function as mRNAs. RNA *10*, 1957-1966.

Carmell, M.A., Xuan, Z.Y., Zhang, M.Q., and Hannon, G.J. (2002). The Argonaute family: tentacles that reach into RNAi, developmental control, stem cell maintenance, and tumorigenesis. Gene Dev *16*, 2733-2742.

Cerutti, H., and Casas-Mollano, J.A. (2006). On the origin and functions of RNA-mediated silencing: from protists to man. Curr Genet *50*, 81-99.

Chai, G., Ma, C., Bao, K., Zheng, L., Wang, X., Sun, Z., Salo, E., Adell, T., and Wu, W. (2010). Complete functional segregation of planarian beta-catenin-1 and -2 in mediating Wnt signaling and cell adhesion. J Biol Chem *285*, 24120-24130.

Chen, C.Z., Li, L., Lodish, H.F., and Bartel, D.P. (2004). MicroRNAs modulate hematopoietic lineage differentiation. Science *303*, 83-86.

Conte, M., Deri, P., Isolani, M.E., Mannini, L., and Batistoni, R. (2009). A mortalin-like

gene is crucial for planarian stem cell viability. Developmental Biology *334*, 109-118.

Eisenhoffer, G.T., Kang, H., and Sanchez Alvarado, A. (2008). Molecular analysis of stem cells and their descendants during cell turnover and regeneration in the planarian Schmidtea mediterranea. Cell Stem Cell *3*, 327-339.

Farrar, G.J., Millington-Ward, S., Chadderton, N., Humphries, P., and Kenna, P.F. (2011). Gene-based therapies for dominantly inherited retinopathies. Gene Ther.

Fernandez-Taboada, E., Moritz, S., Zeuschner, D., Stehling, M., Scholer, H.R., Salo, E., and Gentile, L. (2010). Smed-SmB, a member of the LSm protein superfamily, is essential for chromatoid body organization and planarian stem cell proliferation. Development *137*, 1055-1065.

Friedlander, M.R., Adamidi, C., Han, T., Lebedeva, S., Isenbarger, T.A., Hirst, M., Marra, M., Nusbaum, C., Lee, W.L., Jenkin, J.C.*, et al.* (2009). High-resolution profiling and discovery of planarian small RNAs. Proc Natl Acad Sci U S A *106*, 11546-11551.

Gentile, L., Cebria, F., and Bartscherer, K. (2011). The planarian flatworm: an in vivo model for stem cell biology and nervous system regeneration. Dis Model Mech *4*, 12-19.

Guo, T., Peters, A.H., and Newmark, P.A. (2006). A Bruno-like gene is required for stem cell maintenance in planarians. Dev Cell *11*, 159-169.

Gurley, K.A., Rink, J.C., and Sanchez Alvarado, A. (2008). Beta-catenin defines head versus tail identity during planarian regeneration and homeostasis. Science *319*, 323-327.

Hatfield, S.D., Shcherbata, H.R., Fischer, K.A., Nakahara, K., Carthew, R.W., and Ruohola-Baker, H. (2005). Stem cell division is regulated by the microRNA pathway. Nature *435*, 974-978.

Hayashi, T., Asami, M., Higuchi, S., Shibata, N., and Agata, K. (2006). Isolation of planarian X-ray-sensitive stem cells by fluorescence-activated cell sorting. Development Growth & Differentiation *48*, 371-380.

Hendzel, M.J., Wei, Y., Mancini, M.A., Van Hooser, A., Ranalli, T., Brinkley, B.R., Bazett-Jones, D.P., and Allis, C.D. (1997). Mitosis-specific phosphorylation of histone H3 initiates primarily within pericentromeric heterochromatin during G2 and spreads in an ordered fashion coincident with mitotic chromosome condensation. Chromosoma *106*, 348-360.

Hock, J., and Meister, G. (2008). The Argonaute protein family. Genome Biol *9*, 210.

Hori, I. (1991). Role of fixed parenchyma cells in blastema formation of the planarian

Dugesia japonica. Int J Dev Biol *35*, 101-108.

Hoshi, M., Kobayashi, K., Arioka, S., Hase, S., and Matsumoto, M. (2003). Switch from Asexual to Sexual Reproduction in the Planarian Dugesia ryukyuensis. Integr Comp Biol *43*, 242-246.

Houbaviy, H.B., Murray, M.F., and Sharp, P.A. (2003). Embryonic stem cell-specific MicroRNAs. Dev Cell *5*, 351-358.

Hutvagner, G., and Simard, M.J. (2008). Argonaute proteins: key players in RNA silencing. Nat Rev Mol Cell Biol *9*, 22-32.

Johnston, R.J., and Hobert, O. (2003). A microRNA controlling left/right neuronal asymmetry in Caenorhabditis elegans. Nature *426*, 845-849.

Kim, K., Lee, Y.S., and Carthew, R.W. (2007). Conversion of pre-RISC to holo-RISC by Ago2 during assembly of RNAi complexes. RNA *13*, 22-29.

Lee, Y., Ahn, C., Han, J., Choi, H., Kim, J., Yim, J., Lee, J., Provost, P., Radmark, O., Kim, S.*, et al.* (2003). The nuclear RNase III Drosha initiates microRNA processing. Nature *425*, 415-419.

Lee, Y., Jeon, K., Lee, J.T., Kim, S., and Kim, V.N. (2002). MicroRNA maturation: stepwise processing and subcellular localization. EMBO J *21*, 4663-4670.

Lewis, B.P., Burge, C.B., and Bartel, D.P. (2005). Conserved seed pairing, often flanked

by adenosines, indicates that thousands of human genes are microRNA targets. Cell *120*, 15-20.

Lewis, B.P., Shih, I.H., Jones-Rhoades, M.W., Bartel, D.P., and Burge, C.B. (2003). Prediction of mammalian microRNA targets. Cell *115*, 787-798.

Lillie, F.R. (1900). Some notes on regeneration and regulation in planarians. Am Nat *34*, 173-177.

Liu, J.D., Carmell, M.A., Rivas, F.V., Marsden, C.G., Thomson, J.M., Song, J.J., Hammond, S.M., Joshua-Tor, L., and Hannon, G.J. (2004). Argonaute2 is the catalytic engine of mammalian RNAi. Science *305*, 1437-1441.

Lu, Y.C., Smielewska, M., Palakodeti, D., Lovci, M.T., Aigner, S., Yeo, G.W., and Graveley, B.R. (2009). Deep sequencing identifies new and regulated microRNAs in Schmidtea mediterranea. RNA *15*, 1483-1491.

Miranda, K.C., Huynh, T., Tay, Y., Ang, Y.S., Tam, W.L., Thomson, A.M., Lim, B., and Rigoutsos, I. (2006). A pattern-based method for the identification of MicroRNA binding sites and their corresponding heteroduplexes. Cell *126*, 1203-1217.

Miyoshi, K., Tsukumo, H., Nagami, T., Siomi, H., and Siomi, M.C. (2005). Slicer function of Drosophila Argonautes and its involvement in RISC formation. Genes Dev *19*, 2837-2848.

Morgen, T.H. (1901). regeneration.

Nakagawa, H., Ishizu, H., Hasegawa, R., Kobayashi, K., and Matsumoto, M. (2012). Drpiwi-1 is essential for germline cell formation during sexualization of the planarian Dugesia ryukyuensis. Dev Biol *361*, 167-176.

Naoghare, P.K., Tak, Y.K., Kim, M.J., Han, E., and Song, J.M. (2011). Knock-down of argonaute 2 (AGO2) induces apoptosis in myeloid leukaemia cells and inhibits siRNA-mediated silencing of transfected oncogenes in HEK-293 cells. Basic Clin Pharmacol Toxicol *109*, 274-282.

Newmark, P.A., and Sanchez Alvarado, A. (2002). Not your father's planarian: a classic model enters the era of functional genomics. Nat Rev Genet *3*, 210-219.

Orii, H., Sakurai, T., and Watanabe, K. (2005). Distribution of the stem cells (neoblasts) in the planarian Dugesia japonica. Development Genes and Evolution *215*, 143-157.

Oviedo, N.J., and Levin, M. (2007). smedinx-11 is a planarian stem cell gap junction gene required for regeneration and homeostasis. Development *134*, 3121-3131.

Palakodeti, D., Smielewska, M., and Graveley, B.R. (2006). MicroRNAs from the Planarian Schmidtea mediterranea: a model system for stem cell biology. RNA *12*, 1640-1649.

Palakodeti, D., Smielewska, M., Lu, Y.C., Yeo, G.W., and Graveley, B.R. (2008). The PIWI proteins SMEDWI-2 and SMEDWI-3 are required for stem cell function and piRNA expression in planarians. RNA *14*, 1174-1186.

Palatnik, J.F., Allen, E., Wu, X., Schommer, C., Schwab, R., Carrington, J.C., and Weigel, D. (2003). Control of leaf morphogenesis by microRNAs. Nature *425*, 257-263.

Pearson, B.J., and Sanchez Alvarado, A. (2010). A planarian p53 homolog regulates proliferation and self-renewal in adult stem cell lineages. Development *137*, 213-221.

Petersen, C.P., and Reddien, P.W. (2008). Smed-betacatenin-1 is required for anteroposterior blastema polarity in planarian regeneration. Science *319*, 327-330.

Petersen, C.P., and Reddien, P.W. (2009). A wound-induced Wnt expression program controls planarian regeneration polarity. Proc Natl Acad Sci U S A *106*, 17061-17066.

Randolph, H. (1897). Observations and experiments on regeneration in planarians. Arch Entw Mech Org, 5,352 -355,372.

Reddien, P.W., Bermange, A.L., Kicza, A.M., and Alvarado, A.S. (2007). BMP signaling regulates the dorsal planarian midline and is needed for asymmetric regeneration.

Development *134*, 4043-4051.

Reddien, P.W., Oviedo, N.J., Jennings, J.R., Jenkin, J.C., and Sanchez Alvarado, A. (2005). SMEDWI-2 is a PIWI-like protein that regulates planarian stem cells. Science *310*, 1327-1330.

Rouhana, L., Shibata, N., Nishimura, O., and Agata, K. (2010). Different requirements for conserved post-transcriptional regulators in planarian regeneration and stem cell maintenance. Dev Biol *341*, 429-443.

Sakai, F., Agata, K., Orii, H., and Watanabe, K. (2000). Organization and regeneration ability of spontaneous supernumerary eyes in planarians - Eye regeneration field and pathway selection by optic nerves. Zool Sci *17*, 375-381.

Salo, E., and Baguna, J. (1984). Regeneration and pattern formation in planarians. I. The pattern of mitosis in anterior and posterior regeneration in Dugesia (G) tigrina, and a new proposal for blastema formation. J Embryol Exp Morphol *83*, 63-80.

Salo, E., and Baguna, J. (1989). Regeneration and Pattern-Formation in Planarians .2. Local Origin and Role of Cell Movements in Blastema Formation. Development *107*, 69-76.

Salo, E., and Baguna, J. (2002). Regeneration in planarians and other worms: New findings, new tools, and new perspectives. J Exp Zool *292*, 528-539.

Salvetti, A., Rossi, L., Deri, P., and Batistoni, R. (2000). An MCM2-related gene is expressed in proliferating cells of intact and regenerating planarians. Dev Dyn *218*, 603-614.

Salvetti, A., Rossi, L., Lena, A., Batistoni, R., Deri, P., Rainaldi, G., Locci, M.T., Evangelista, M., and Gremigni, V. (2005). DjPum, a homologue of Drosophila Pumilio, is essential to planarian stem cell maintenance. Development *132*, 1863-1874.

Schwarz, D.S., Hutvagner, G., Du, T., Xu, Z., Aronin, N., and Zamore, P.D. (2003). Asymmetry in the assembly of the RNAi enzyme complex. Cell *115*, 199-208.

Scimone, M.L., Meisel, J., and Reddien, P.W. (2010). The Mi-2-like Smed-CHD4 gene is required for stem cell differentiation in the planarian Schmidtea mediterranea. Development *137*, 1231-1241.

Slack, J.M. (1980). The source of cells for regeneration. Nature *286*, 760.

Slack, J.M. (2011). Development. Planarian pluripotency. Science *332*, 799-800.

Solana, J., Lasko, P., and Romero, R. (2009). Spoltud-1 is a chromatoid body component required for planarian long-term stem cell self-renewal. Dev Biol *328*, 410-421.

Song, J.J., Smith, S.K., Hannon, G.J., and Joshua-Tor, L. (2004). Crystal structure of

Argonaute and its implications for RISC slicer activity. Science *305*, 1434-1437.

Suh, M.R., Lee, Y., Kim, J.Y., Kim, S.K., Moon, S.H., Lee, J.Y., Cha, K.Y., Chung, H.M., Yoon, H.S., Moon, S.Y*., et al.* (2004). Human embryonic stem cells express a unique set of microRNAs. Dev Biol *270*, 488-498.

Tabara, H., Yigit, E., Siomi, H., and Mello, C.C. (2002). The dsRNA binding protein RDE-4 interacts with RDE-1, DCR-1, and a DExH-box helicase to direct RNAi in C. elegans. Cell *109*, 861-871.

Tamura, S., Yamamoto, K., Takai, M., Oki, I., and Kawakatsu, M. (1998). Karyology and biogeography of Dugesia japonica and Dugesia ryukyuensis in Kyushu, southern Japan. Hydrobiologia *383*, 321-327.

Tian, Q.N., Bao, Z.X., Lu, P., Qin, Y.F., Chen, S.J., Liang, F., Mai, J., Zhao, J.M., Zhu, Z.Y., Zhang, Y.Z*., et al.* (2011). Differential expression of microRNA patterns in planarian normal and regenerative tissues. Mol Biol Rep.

Umesono, Y., Tasaki, J., Nishimura, K., Inoue, T., and Agata, K. (2011). Regeneration in an evolutionarily primitive brain--the planarian Dugesia japonica model. Eur J Neurosci *34*, 863-869.

Wagner, D.E., Wang, I.E., and Reddien, P.W. (2011). Clonogenic neoblasts are pluripotent adult stem cells that underlie planarian regeneration. Science *332*,

811-816.

Yan, K.S., Yan, S., Farooq, A., Han, A., Zeng, L., and Zhou, M.M. (2003). Structure and conserved RNA binding of the PAZ domain. Nature *426*, 468-474.

Yoshida-Kashikawa, M., Shibata, N., Takechi, K., and Agata, K. (2007). DjCBC-1, a conserved DEAD box RNA helicase of the RCK/p54/Me31B family, is a component of RNA-protein complexes in planarian stem cells and neurons. Dev Dyn *236*, 3436-3450.

Yuan, Y.R., Pei, Y., Ma, J.B., Kuryavyi, V., Zhadina, M., Meister, G., Chen, H.Y., Dauter, Z., Tuschl, T., and Patel, D.J. (2005). Crystal structure of A. aeolicus argonaute, a site-specific DNA-guided endoribonuclease, provides insights into RISC-mediated mRNA cleavage. Mol Cell *19*, 405-419.

A

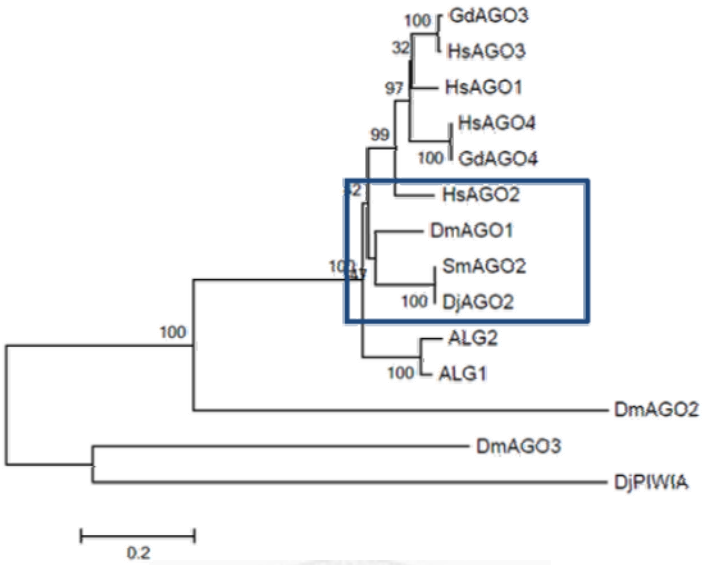
GdAGO3
HsAGO3
HsAGO1
HsAGO4
GdAGO4
HsAGO2
DmAGO1
SmAGO2
DjAGO2
ALG2
ALG1
DmAGO2
DmAGO3
DjPIWIA
100
32
97
99
100
92
100
100
100
100
0.2

B


N
PAZ domain
Mid domain
PIWI domain
DjAgo2 MLGGTYFTPP TYLFNSNGNS ENNNNTLCLA STPNGNQTMN PLGAPGQPPN TSVPAIIGST 60
HsAgo2 MYSGA----- ---------- ---------- ---------G PALAPPAPP- ---PPIQG-- 20
DjAgo2 QLSSNLSSGP SPPQLPTGSN SQYSSSGNGS VYFQPPSRPD QGTDGRTIQL KANHFEIVMP 120
HsAgo2 ---------- ---------- --YA------ --FKPPPRPD FGTSGRTIKL QANFFEMDIP 50
DjAgo2 KGFLHHYDIT ITPEKCPRRV NRDIIQAMVN NMHYQKYFYN QKPVFDGRRN MYTREPLSIG 180
HsAgo2 KIDIYHYELD IKPEKCPRRV NREIVEHMVQ HFKTQ-IFGD RKPVFDGRKN LYTAMPLPIG 108
DjAgo2 KEKLELEVIL PGEGKDRVFK VCLKHVSEVS LFALEEALQG RRQTIPAETV TALDVIMRHL 240
HsAgo2 RDKVELEVTL PGEGKDRIFK VSIKWVSCVS LQALHDALSG RLPSVPFETI QALDVVMRHL 169
DjAgo2 PSMTYTPVGR SFFHNTGDYD NPLGGGREVW FGFHQSVRPS QWKMMLNIDV SATAFYKEQS 300
HsAgo2 PSMRYTPVGR SFFTASEGCS NPLGGGREVW FGFHQSVRPS LWKMMLNIDV SATAFYKAQP 229
DjAgo2 VINFMFEVLE ID--KDLKRP LTDSQRVKFT KEIKGLKVEI NHCGPIKRKY RVCNVTRRSA 358
HsAgo2 VIEFVCEVLD FKSIEEQQKP LTDSQRVKFT KEIKGLKVEI THCGQMKRKY RVCNVTRRPA 288
DjAgo2 QSQTFPLQSE QGQTIECTVT KYFQDRYGMK LQHPHLPCLQ VGQEQKHTYL PLEVCNIVSG 418
HsAgo2 SHQTFPLQQE SGQTVECTVA QYFKDRHKLV LRYPHLPCLQ VGQEQKHTYL PLEVCNIVAG 349
DjAgo2 QRCIKKLTDM QTSTMIKATA RSAPDREKEI NNLVRRSNFN ADPHLQIFGV SVNTRMADIQ 478
HsAgo2 QRCIKKLTDN QTSTMIRATA RSAPDRQEEI SKLMRSASFN TDPYVREFGI MVKDEMTDVT 409
DjAgo2 GRVIPAPKIQ YGGRTKAQAT PQQGVWDMRG KQFFSGIEIK VWAIACFAPQ RTVREDSLRT 538
HsAgo2 GRVLQPPSIL YGGRNKAIAT PVQGVWDMRN KQFHTGIEIK VWAIACFAPQ RQCTEVHLKS 468
DjAgo2 FTQQLQKISN DAGMPIVGQP CFCKYATGQD QVEPMFRYLK NSFSGLQLIV VVLPGKTPVY 598
HsAgo2 FTEQLRKISR DAGMPIQGQP CFCKYAQGAD SVEPMFRHLK NTYAGLQLVV VILPGKTPVY 529
DjAgo2 AEVKRVGDII FGLATQCVQA KNVNKPSPQT LSNLCLKINV KLGGINSILV PSVRPAVFKE 658
HsAgo2 AEVKRVGDTV LGMATQCVQM KNVQRTTPQT LSNLCLKINV KLGGVNNILL PQGRPFFVFQQ 589
DjAgo2 PVIFLGADFT HPPAGDKTKP SIAAVVGSMD AHPSRYAATV SVQPHRQETI QDLAAMVKEL 718
HsAgo2 PVIFLGADVT HPPAGDQKKP SIAAVVGSMD AHPNRYCATV RVQQHRQEII QDLAAMVREL 649
DjAgo2 LIQFYKSTRF KPTRIIYYRD GVSEGQFLNV LNHELKAIRE ACIKLEMSYQ PGITFVVVQK 778
HsAgo2 LIQFYKSTRF KPTRIIFYRD GVSEGQFQQV LHHELLAIRE ACIKLEKDYQ PGITFIVVQK 709
DjAgo2 RHHTRLFCSD KKDQMGRSGN IPAGTTVDQI ITHPTEFDFY LCSHAGIQGT SRPSHYHVLW 838
HsAgo2 RHHTRLFCTD KNERVGKSGN IPAGTTVDTK ITHPTEFDFY LCSHAGIQGT SRPSHYHVLW 768
DjAgo2 DDNRFSADEI QTLTYQLCHT YVRCTRSVSI PAPAYYAHLV AFRARYHLVE KELDSQEGSQ 898
HsAgo2 DDNRFSSDEL QILTYQLCHT YVRCTRSVSI PAPAYYAHLV AFRARYHLVD KEHDSAEGSH 829
DjAgo2 KSGNSDERNP TAMMRAVTVH SETLKVMYFA * 929
HsAgo2 TSGQSNGRDH QALAKAVQVH QDTLRTMYFA * 860

Figure1. (A) Phylogenetic analysis of *Dj*Ago2 and Argonaute subfamily. Phylogenetic tree was constructed by neighbor-joining algorithm. *Dj*Ago2 belongs to Argonaute subfamily and closely related to *S. mediterranea* Ago2, *Drosophila* Ago1 and human Ago2 (blue frame). *Dm*Ago3 and *Dj*PiwiA are member of the PIWI subfamily. Scale bar: 20% amino acid substitutions. (B) Sequence alignment of *Dj*Ago2 and human Ago2 (*hs*Ago2). *Dj*Ago2 exhibits high similarity to human Ago2 with 76.5% identity. *Dj*Ago2 contains the conserved N-terminal, PAZ, Mid, and PIWI domains, as well as the catalytic residues (blue frames).

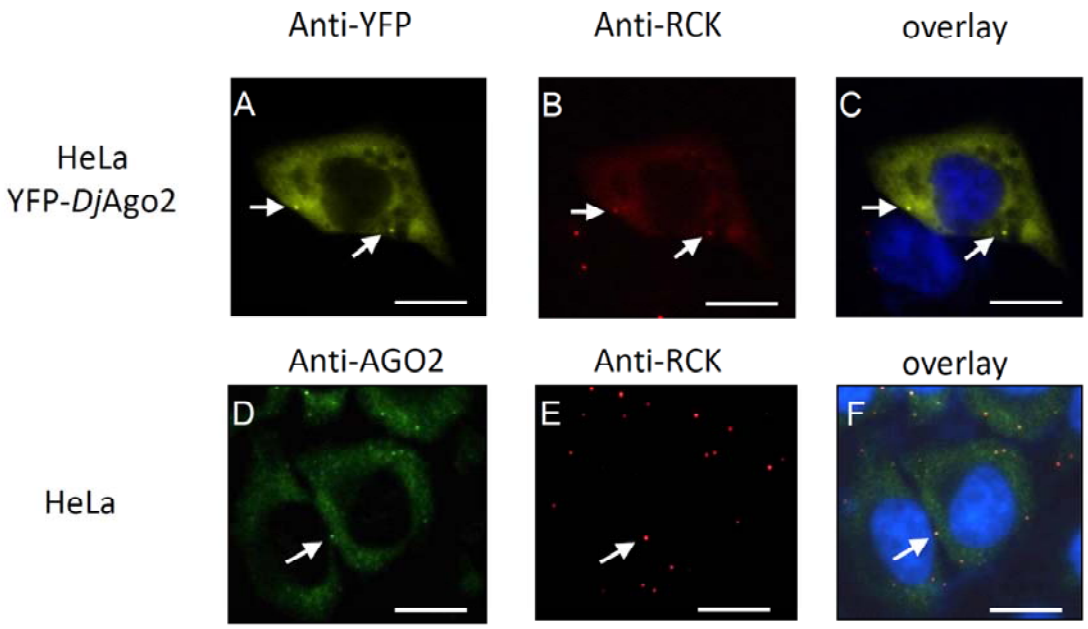

Figure 2. *Dj*Ago2 accumulates at specific foci (white arrow) in the cytoplasm and co-localizes with RCK/p54, a marker for RNA processing (P-) body. HeLa cells transfected with YFP-*Dj*Ago2 were fixed at 24h post-transfection. Immunofluorescence analysis of YFP-*Dj*Ago2 was performed with mouse anti-YFP antibody followed by alexa-488-conjugated anti-mouse IgG (panel A). HeLa cells were co-stained with rabbit anti-RCK followed by alexa-568-conjugated anti-rabbit IgG (panel B, E). Nucleus were labeled with Hoechst 33342. Subcellular localization of *Dj*Ago2 is similar to that of *hs*Ago2 (panels D-F). Immunofluorescence analysis of endogenous *hs*Ago2 was performed with mouse anti-Ago2 antibody followed by Alexa-488-conjugated anti-mouse IgG (panel D). Scale bar: 10μm.

A

B

Figure 3. Expressions of *Djago2* and *DjpiwiA* at the dorsal middle line of planarian. (A) Expression of *Djago2*. *In situ* hybridization of *Djago2* was performed with a ~1.5-kb anti-sense RNA probe. *Djago2* is highly expressed in brain region (black arrow) and dorsal line (black arrow head), and these signals were absent from control animals (sense probe). Scale bar: 1.5 mm. (B) Expression pattern of *DjpiwiA* in intact animals. *DjpiwiA* is a neobalst marker, and is primarily expressed on the dorsal middle line (yellow arrow head). A ~2.5-kb anti-sense RNA probe was used. Scale bar: 1.5 mm.

A

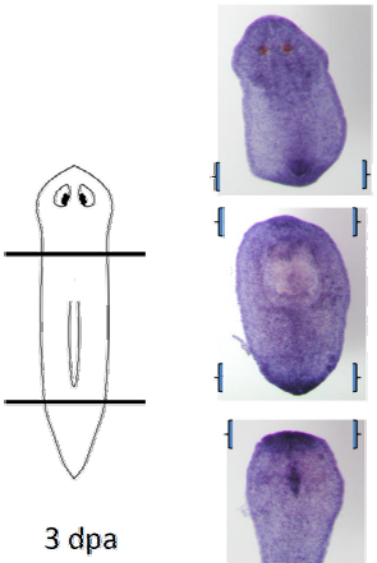

B

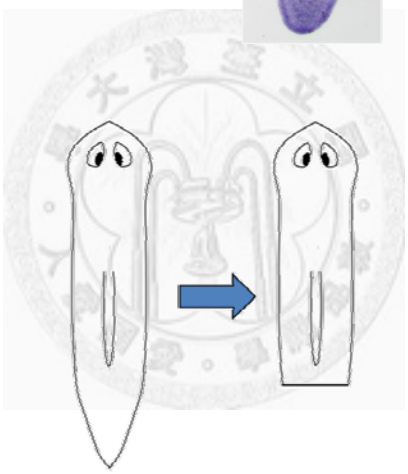

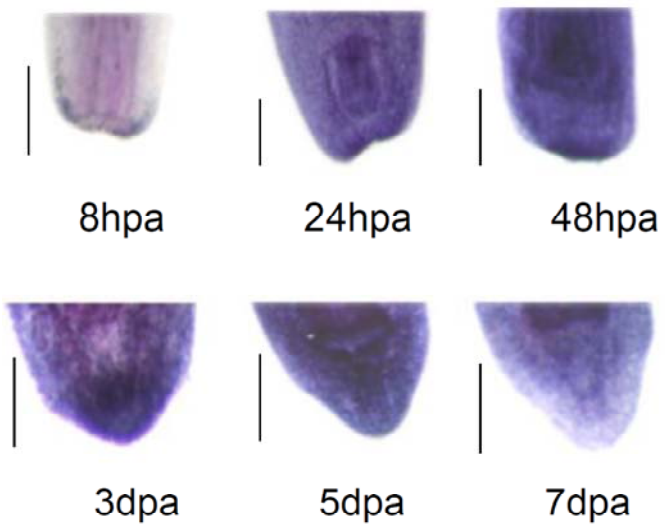

Figure 4. Expression of *Djago2* is increased in regenerating regions. (A) Expression pattern of *Djago2* in regenerating fragments. Worms are harvested and analyzed on day 3 after transverse amputation at anterior or posterior of the pharynx. The level of *Djago2* mRNA is increased in both head and tail regenerating regions (parentheses). (B) Expression of *Djago2* at various time points during tail regeneration. The increased level of *Djago2* in regenerating tissue was observed from 24hpa to 3dpa. Scale bar: 80 μm.

A

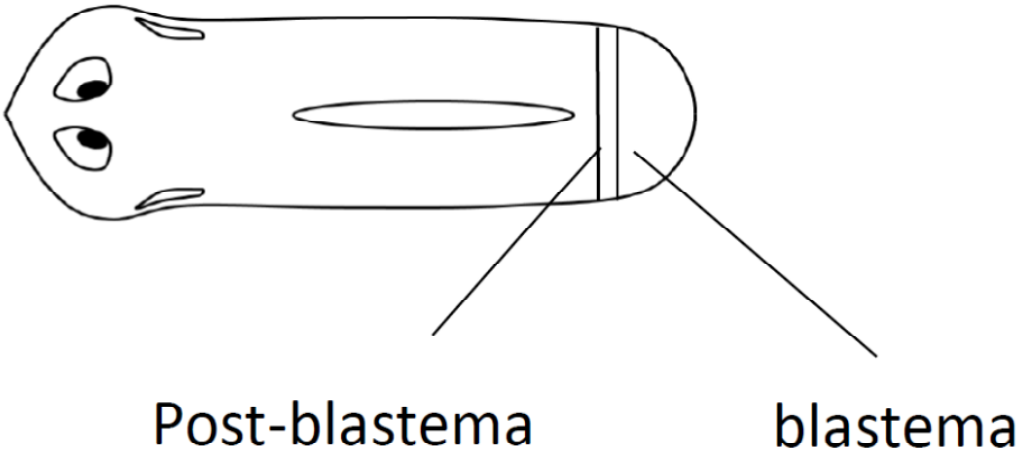
Post-blastema
blastema

B

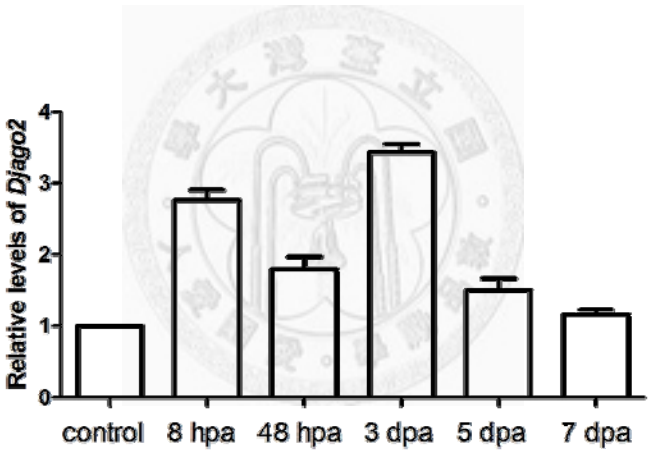
Relative levels of Djago2
0
1
2
3
4
control
8 hpa
48 hpa
3 dpa
5 dpa
7 dpa

C

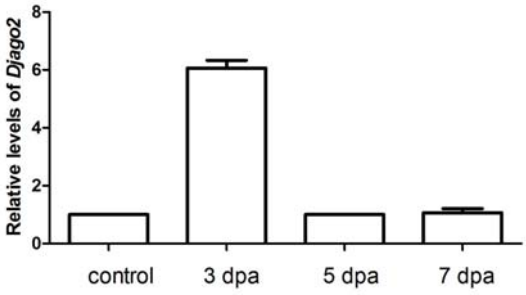
Relative levels of Djago2
0
2
4
6
8
control
3 dpa
5 dpa
7 dpa

D

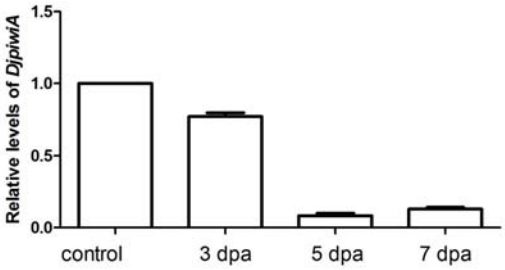
Relative levels of DjpiwiA
0.0
0.5
1.0
1.5
control
3 dpa
5 dpa
7 dpa

Figure 5. Quantitative analysis of *Djago2* expression during regeneration. (A) New formed tissue without pigment was collected as blastema. The region next to the blastema is post-blastema. (B) Quantitative analysis of *Dj*ago2 expression at post-blastema during regeneration by RT-qPCR. The levels of *Djago2* mRNA for various time points after amputation were normalized to actin and are presented as relative to that in control (same region of worm body before amputation). The peak level of *Djago2* was observed on day 3 post-amputation. (C) Expression of *Djago2* in bastema. Highest level of *Djago2* in blastema was observed on day 3 post-amputation. (D) Expression of *DjpiwiA* is reduced in blastema. Expression of *DjpiwiA* was analysis by RT-QPCR. Levels of *DjpiwiA* were normalized to that of actin and are presented as relative to that in control.

A


Normal
Irradiated

B

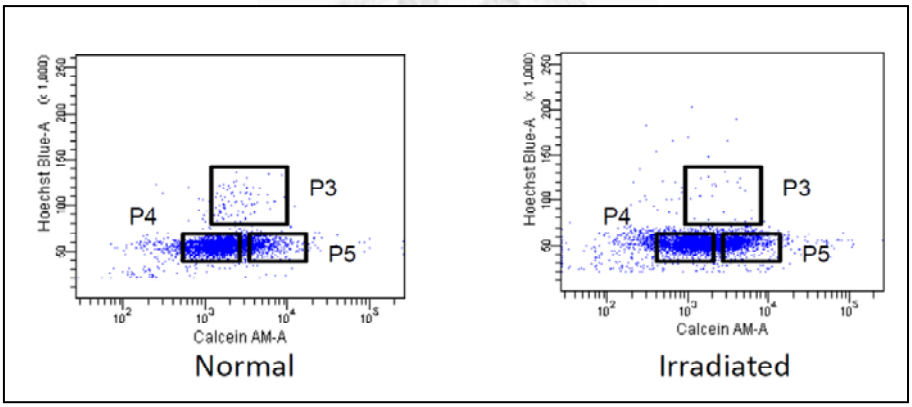
Hoechst Blue-A
Calcein AM-A
P3
P4
P5
Normal
Irradiated

C

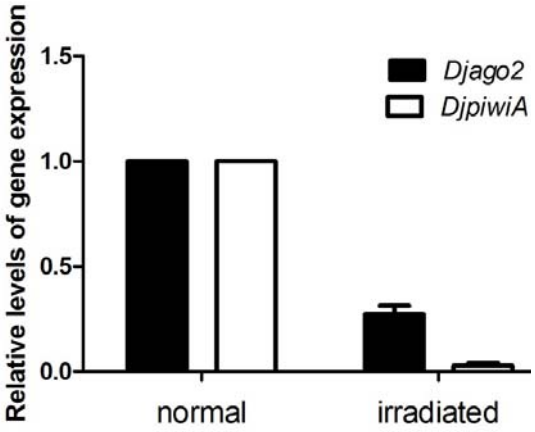
Relative levels of gene expression
1.5
1.0
0.5
0.0
Djago2
DjpiwiA
normal
irradiated

Figure 6. Expression of *Djago2* is reduced in γ-irradiated planarians. (A) γ-irradiation induces the defect on homeostasis in planarians. Fifteen worms were treated with 90Gy and the head regression phenotype was observed on Day 14 after γ-irradiation. All animals were dead in 3 to 4 weeks after irradiation. (B) Depletion of neoblasts by γ-irradiation. Cells from dissociated animals were stained with Hoechst 33342 and Calcein-*AM*. P3 regions indicate the population of neoblasts with high nucleus/cytosol ratio. The numbers of neoblasts in irradiated worms were significantly reduced as compared to that in normal worms. (C) Quantitative analysis of *Djago2* and *DjpiwiA* in irradiated planarians. Total RNAs collected from three worms on day 3 post-irradiation were reverse transcribed and subjected to quantitative PCR to analyze the level of *DjpiwiA* (a neoblast marker gene) and *Djago2*, as comparing with that in un-irradiated worms. Our data shows that γ-irradiation indeed eliminated the *DjpiwiA*-positive cells, the neoblasts, and reduced the *Djago2* level as well.

A

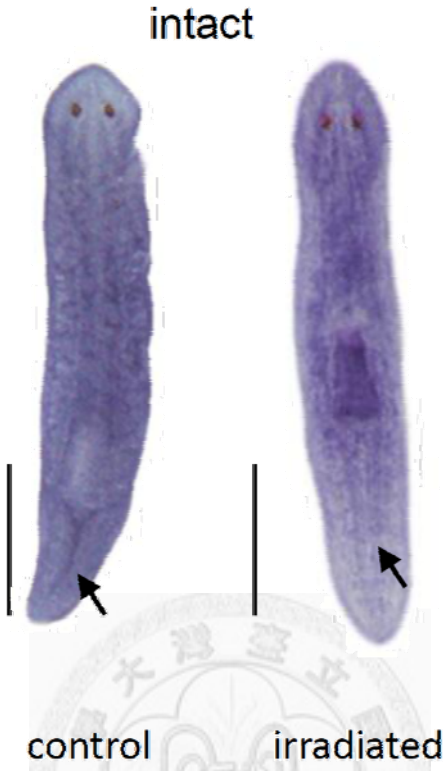

B

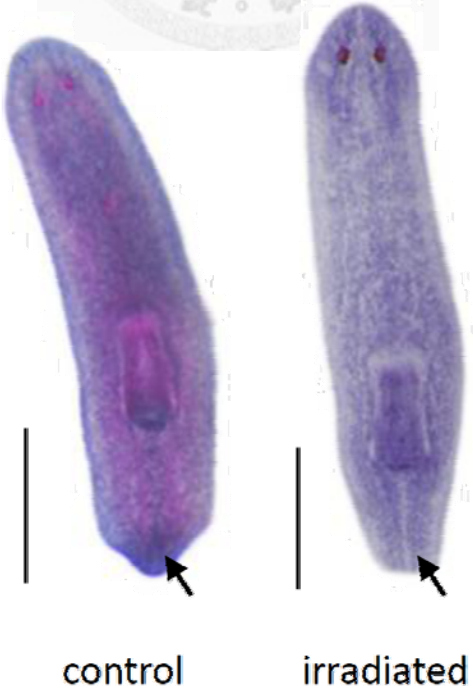

Figure 7. Elimination of *Djago2*-positive cells at regenerating tissue by γ-irradiation. (A) Expression of *Djago2* at dorsal middle line, where the neoblasts concentrated (white arrowhead), was abolished in irradiated animals, while signals of *Djago2* in CNS remained unaffected. Scale bar: 1.5 mm. (B) Expression of *Djago2* in regenerating animals with γ-irradiation. No significant increase of *Djago2* at the wound site on day 3 post-amputation in γ-irradiated animals. Scale bar: 1.5 mm.

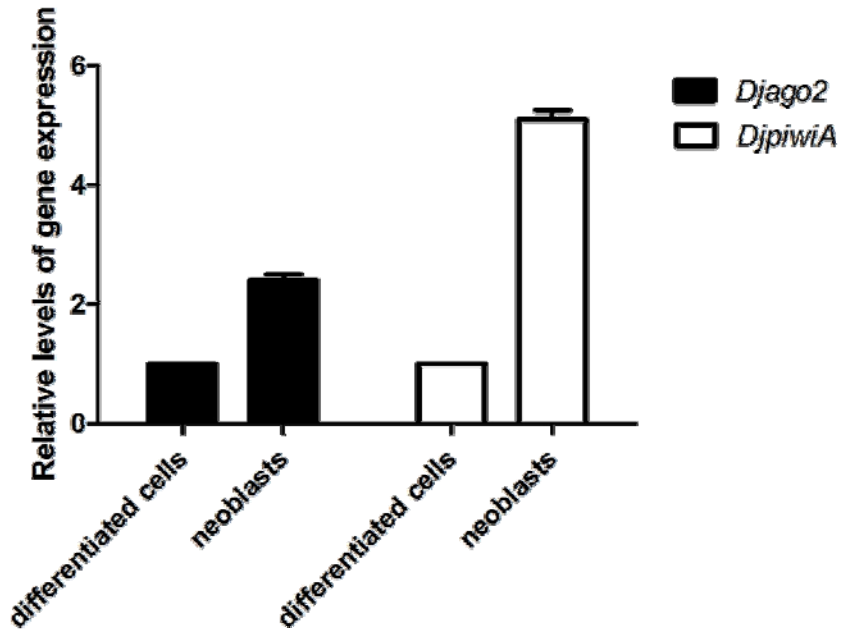

Figure 8. Quantitative analysis of *Djago2* and *DjpiwiA* mRNA levels in neoblasts and differentiated cells isolated from single-cell suspensions. Single-cell suspensions were prepared by dissociating small pieces of planarians with trypsin treatment, gentle pipetting, and then filtering through 70-μm and 20-μm filters. Cells were stained with Hoechst 33342 and Calcein-*AM*, and subjected to FACS analysis as described in Fig 6. Cells from P3 region (neoblasts) and P5 region (differentiated cells), as described in figure 6B, were isolated for RT-qPCR analysis to compare to expression levels of *Djago2* and *DjpiwiA*. The level of *Djago2* in neoblasts was about two folds higher than that in in differentiated cells. *DjpiwiA,* which is highly expressed in neoblasts, was used as the positive control of neoblasts specific genes.

A

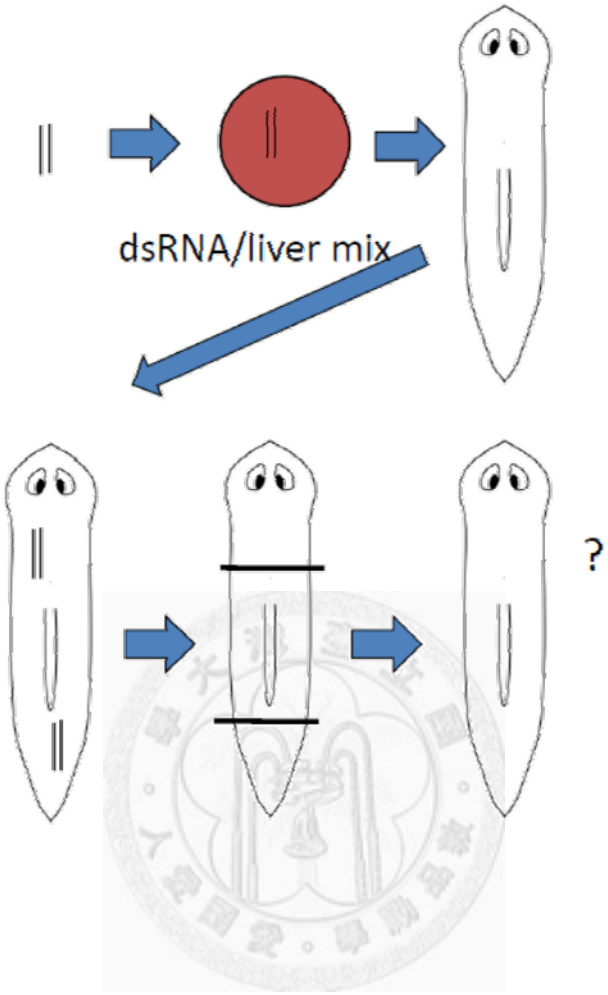

B

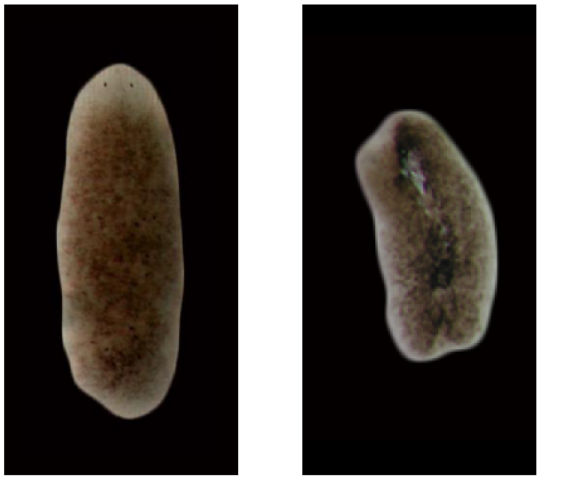

C

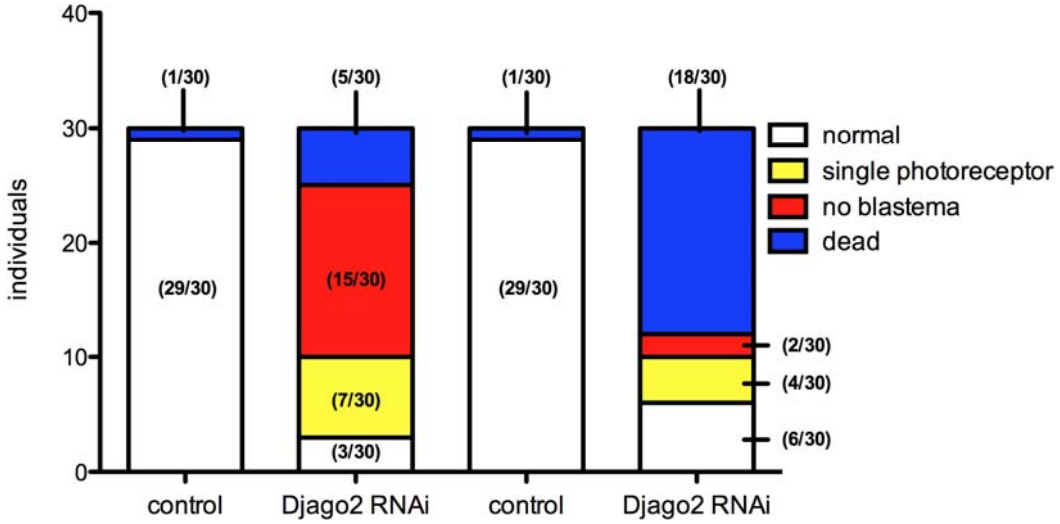
40
30
20
10
0
individuals
(1/30)
(5/30)
(1/30)
(18/30)
(29/30)
(15/30)
(29/30)
(7/30)
(3/30)
(2/30)
(4/30)
(6/30)
normal
single photoreceptor
no blastema
dead
control
Djago2 RNAi
control
Djago2 RNAi

D

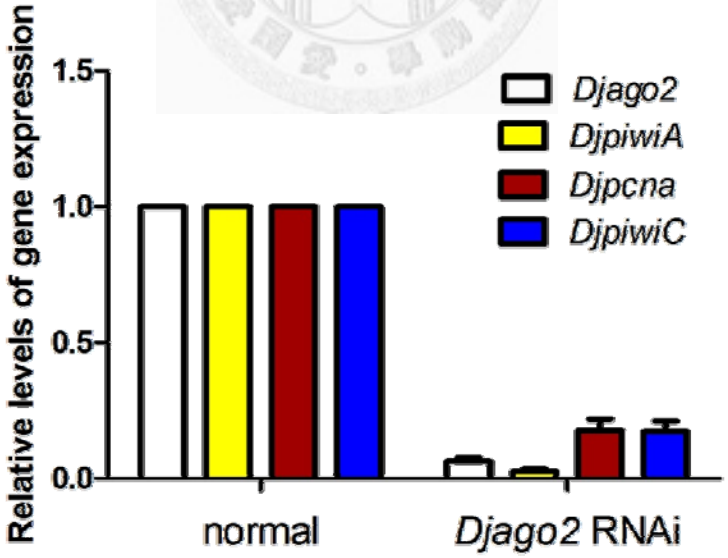
Relative levels of gene expression
1.5
1.0
0.5
0.0
Djago2
DjpiwiA
Djpcna
DjpiwiC
normal
Djago2 RNAi

E

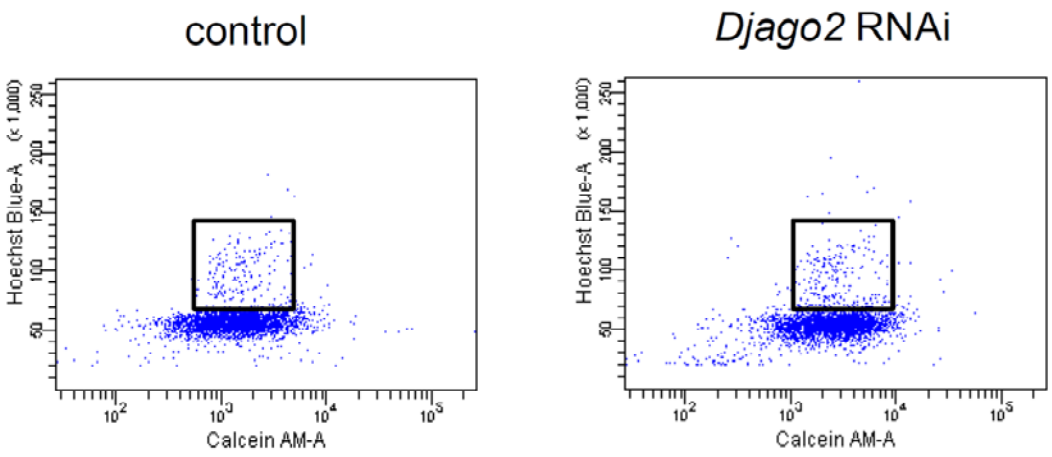
control
Djago2 RNAi
Hoechst Blue-A (x 1,000)
Calcein AM-A

F

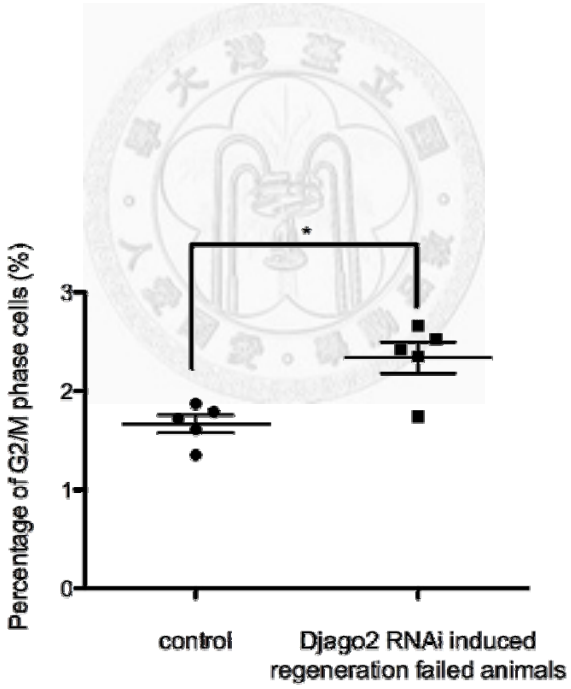
Percentage of G2/M phase cells (%)
*
control
Djago2 RNAi induced regeneration failed animals

Figure 9. *Djago2* is required for planarian regeneration and neoblasts homeostasis. (A) Experimental outline of *Djago2* silencing in planarian. *In vitro* transcribed *Djago2* dsRNA was purified and mixed with chicken liver in low-melting agarose gel for feeding RNAi. (B). *Djago2* RNAi induces the deficiency in regeneration. For one round of RNAi treatment, each worm was fed with dsRNA/liver mix (4mg dsRNA in 25μl chicken liver) on Day 1, 4, and 7, followed by transverse amputation at the sites anterior or posterior to pharynx on Day 10 to remove the head and tail regions. The phenotype in *Djago2* RNAi-treated samples was examined on 7 days after completing one rounds of RNAi. I observed the loss of head and tail regenerations in planarians fed with *Djago2* RNAi, but not in controls (YFP RNAi). (C) *Djago2* silencing led to failed or limited regeneration. Phenotypes of control (YFP RNAi) and *Djago2* silenced animals were inspected on Day 7 and Day 14 post amputation (dpa). Ratios of animals for each phenotype in control or *Djago2* RNAi samples are labeled. (D) *Djago2* silencing also reduced the levels of *DjpiwiA, DjPCNA, and DjpiwiC*. Total RNA extracted from control or *Djago2* RNAi animals was analyzed by RT-qPCR to quantify the levels of various neoblast-related genes, including *DjpiwiA* and *DjpiwiC* (neoblasts-specific) and *DjPCNA* (S phase-specific). (E) FACS analysis of single-cell suspensions from planarians treated with *Djago2* RNAi. The ratio of G2/M phase cells was not reduced in *Djago2* RNAi animals as compared to that in control. Planarian cells were stained with Hoechst 33342 and Calcein-*AM* and analyze by FACS as described before. (F) Quantitation of G2/M-phase cells in (D). The percentage of G2/M phase cells was increased in regeneration-failed animals with RNAi against *Djago2*.

A

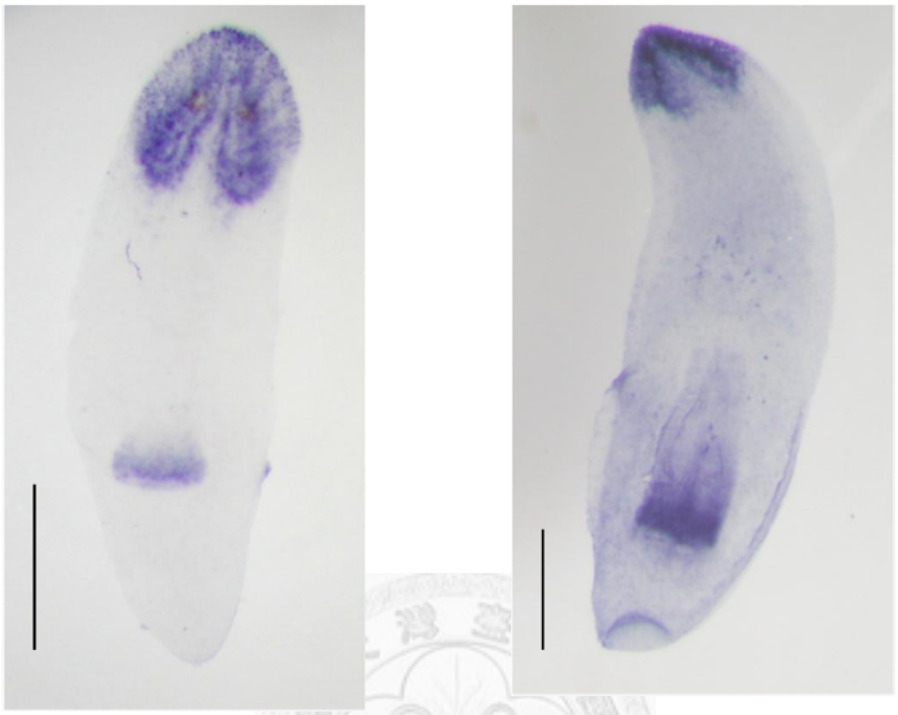

Figure 10. Limited head regeneration was observed in *Djago2* silenced animals. Some specimens (*Djago2* RNAi-treated trunks) incompletely regenerate their new heads with only one photoreceptor on Day 14 post-amputation. By using *in situ* hybridization, *Djndk* specifically labeled the brains of regenerated animals. It shows that the brain size was significantly reduced under *Djago2* RNAi treatment. Scale bar: 1 mm.

A


control
Djago2 RNAi

B

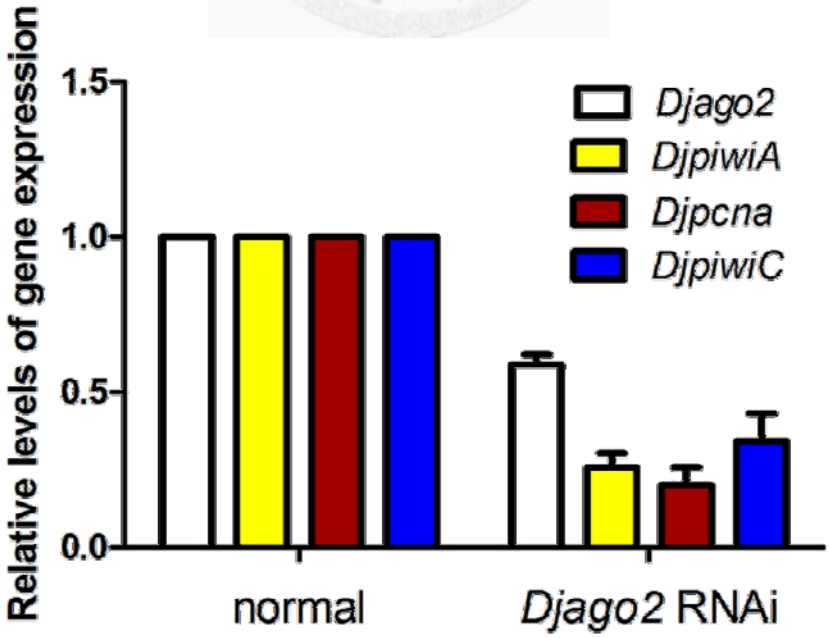
Relative levels of gene expression
1.5
1.0
0.5
0.0
Djago2
DjpiwiA
Djpcna
DjpiwiC
normal
Djago2 RNAi

C

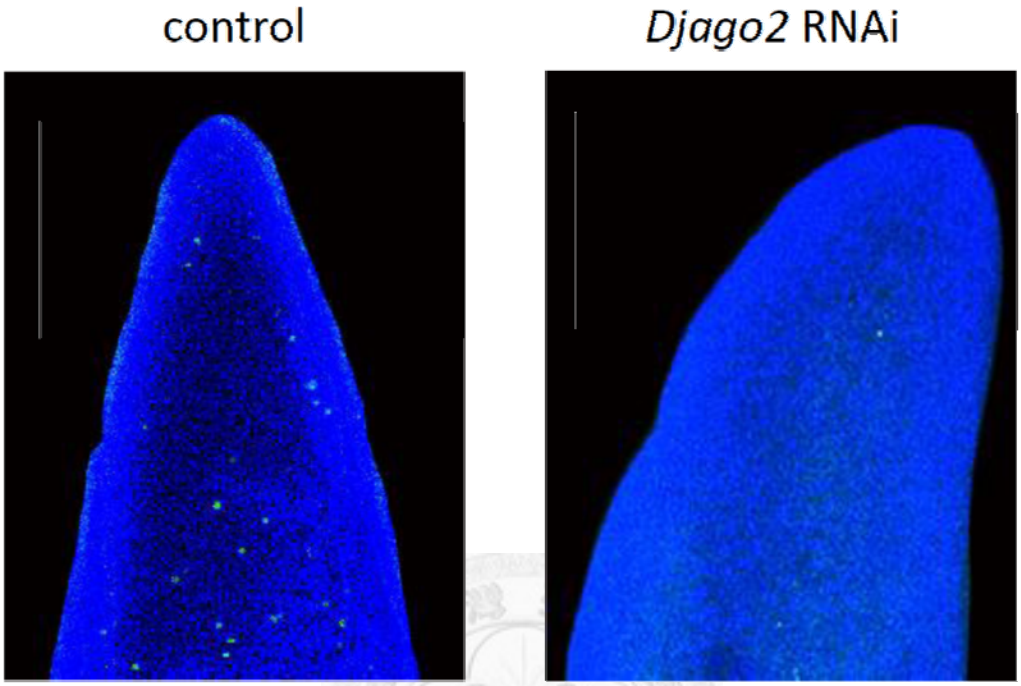
control
Djago2 RNAi

D

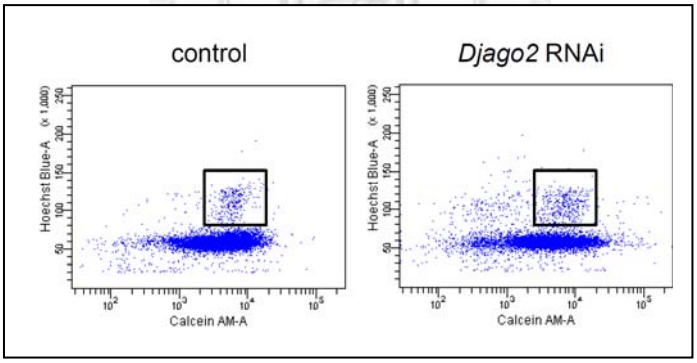
control
Djago2 RNAi
Hoechst Blue-A
Calcein AM-A

E

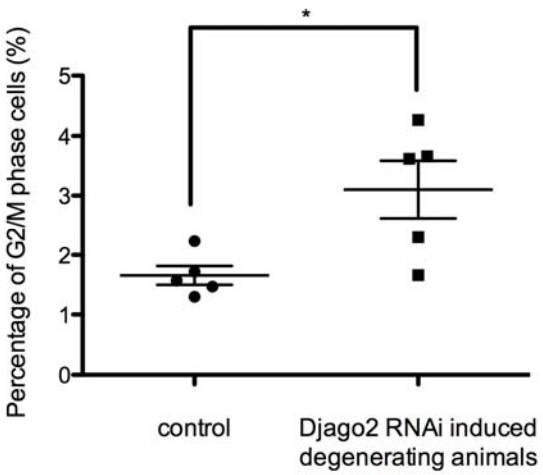
*
Percentage of G2/M phase cells (%)
0
1
2
3
4
5
control
Djago2 RNAi induced degenerating animals

Figure 11. *Djago2* RNAi induces the defect on homeostasis. (A). The phenotype of *Djago2* RNAi-treated samples was examined on day 10 after finishing one round of RNAi treatment (6mg dsRNA in 25μl chicken liver). A significant head-regression phenotype was observed in *Djago2* RNAi animals. The animals with *Djago2* RNAi exhibited a continuous regression phenotype even the RNAi treatment has been stopped for 1 week. (B) Silencing of *Djago2* reduced the levels of *DjpiwiA, DjPCNA, and DjpiwiC.* in degenerating worms. Total RNA from control or degenerating animals was analyzed by RT-qPCR to quantify the levels of various neoblast-related genes, including *DjpiwiA* and *DjpiwiC* (neoblasts-specific) and *DjPCNA* (S phase-specific). Results showed that neoblasts were depleted in *Djago2*-RNAi animals and resulted in the tissue degeneration. (C) The number of mitotic cells was reduced in *Djago2* RNAi animals. During mitosis, serine 10 of histone H3 becomes phosphorylated throughout condensing chromatin. We used anti-H3p antibody to label the mitotic cells (yellow) and Hoechst 33342 to label cell nuclear (blue). We observed the reduced amounts of mitotic cells in *Djago2*-RNAi worms (right panel) as compared to control. Scale bar: 200 μm. (D) FACS analysis of single cell suspension from degenerating planarians treated with *Djago2* RNAi. The ratio of G2/M-phase cells was not reduced in degenerating animals. Planarian cells were stained with Hoechst 33342 and Calcein-*AM* and analyzed by FACS (BD AriaIII) as described above. (E) The percentage of G2/M-phase cells was increased in degenerating animals. Quantitation of G2/M-phase cells from FACS results. In each group, 5 animals were subjected for preparing the single cells suspension individually. Our data indicates the increasing amounts of G2/M cells in degenerating animals. (*$p < 0.05$)

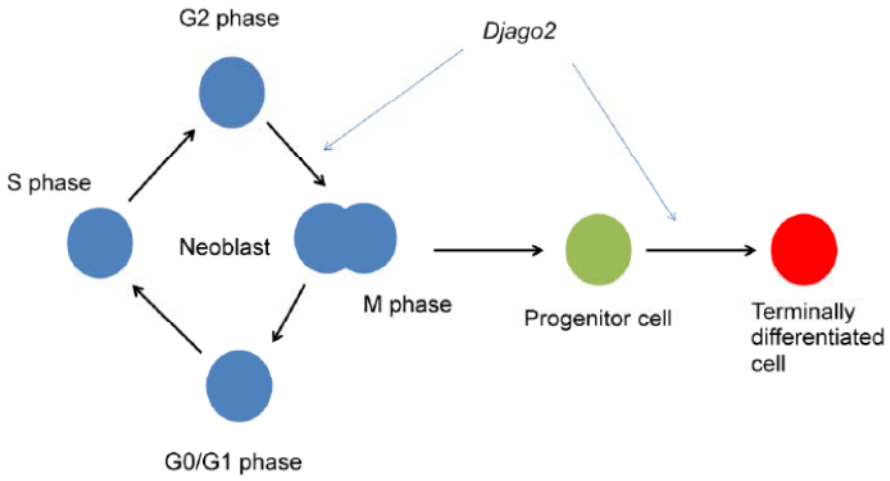

Figure 12. Model for the regulation of *Djago2* in neoblast proliferation and differentiation. In planarians, neoblasts aggregate and proliferate in the post-blastema, and dividing progeny aggregate and differentiate in the blastema during regeneration. In this study, my results suggested that *Djago2* can regulate the cell cycle of neoblasts from the G2 to the M phase, and *Djago2* is required for the differentiation of progenitor cells.